



**Politecnico
di Torino**

Politecnico di Torino

Master of Science in Environmental and Land Engineering
A.y. 2023/2024

Development of a Life Cycle Inventory (LCI) for the environmental assessment of Vanadium redox flow batteries

Supervisors:

Eng. Isabella Bianco
Prof.ssa Deborah Panepinto
Prof. Giovanni Andrea Blengini

Candidate:

Andrea Faldi

Summary

| | |
|--|----|
| 1. Introduction..... | 2 |
| 1.1. The global warming: origins and possible strategies to mitigate it | 2 |
| 1.2. Stationary batteries and goal of this thesis | 4 |
| 2. Technology of batteries | 5 |
| 2.1. Electrochemical energy storage: how it works and which types exist | 5 |
| 2.2. Redox batteries for stationary applications | 6 |
| 2.3. Vanadium redox flow batteries..... | 7 |
| 2.4. Optimization of VRFB over the years | 11 |
| 3. Life Cycle Assessment (LCA) | 13 |
| 3.1. LCA methodology..... | 13 |
| 3.2. LCA of batteries in the European framework..... | 14 |
| 4. State of art on LCA of Vanadium redox flow batteries | 16 |
| 4.1. System boundaries | 17 |
| 4.2. Functional unit and source of data..... | 17 |
| 4.3. Phases of Vanadium batteries life cycle..... | 18 |
| 4.3.1. Material extraction | 18 |
| 4.3.2. Manufacturing and assembly | 18 |
| 4.3.3. Use phase | 19 |
| 4.3.4. End-of-Life and recycling | 20 |
| 4.3.5. Transportation | 20 |
| 4.4. Sensitivity analysis..... | 21 |
| 5. ENVIRONMENTAL LIFE CYCLE ASSESSMENT OF VRFB | 24 |
| 5.1. Goal and scope | 24 |
| 5.2. Life cycle inventory (LCI) | 24 |
| 5.2.1. Battery manufacturing (production phase) | 25 |
| 5.2.2. Life cycle inventory for the manufacturing and transportation of VRFB | 45 |
| 5.2.3. Use phase | 46 |
| 5.2.4. End-of-life phase | 48 |
| 5.2.5. Final LCI for Vanadium Redox Flow Battery | 50 |
| 5.3. Life cycle impact assessment (LCIA) | 51 |
| 6. DISCUSSION | 58 |
| 7. Conclusions | 60 |
| BIBLIOGRAPHY | 61 |

1. Introduction

1.1. The global warming: origins and possible strategies to mitigate it

Nowadays, fossil fuels are widely used for meeting energy needs of human society but this has a huge impact, “not only environmental (e.g. climate change) but also economical and even social (e.g. supply security)” [1]. The red line in Figure 1 represents the average land-sea temperature oscillations trend compared to the 1961-1990 average temperature, with upper and lower confidence intervals shown in light grey. It’s possible to note that over the last decades, global temperatures have risen sharply — to about 0.7°C (Our world in Data). The Intergovernmental Panel on Climate Change (IPCC) states clearly in its AR5 assessment report:

“Anthropogenic greenhouse gas emissions have increased since the pre-industrial era, driven largely by economic and population growth, and are now higher than ever. This has led to atmospheric concentrations of carbon dioxide, methane and nitrous oxide that are unprecedented in at least the last 800’000 years. Their effects, together with those of other anthropogenic drivers, have been detected throughout the climate system and are extremely likely to have been the dominant cause of the observed warming since the mid-20th century” (Intergovernmental Panel on Climate Change).

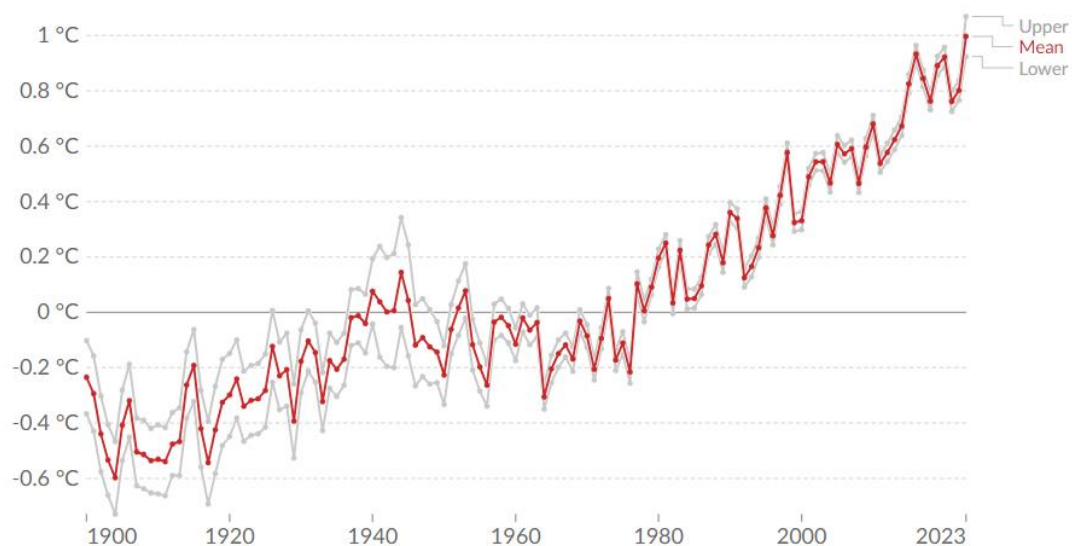


Figure 1 - Average global temperature anomaly (Our world in Data)

For this reason several stakeholders are promoting the use of energy from renewable sources, in particular, the European Commission has adopted a set of proposals to transform EU in terms of climate, energy, transport and taxation policies, with the aim of reducing net greenhouse gas emissions by at least 50% by 2030, compared to 1990 levels (European Green Deal) and achieve carbon neutrality in the continent by 2050. The studies suggest that the share of renewable in EU energy mix will increase to 25% by 2030 and at least 35% by 2050 [1]. According to the strategic research provider BNEF (Bloomberg New Energy Finance) starting in 2018 and moving forward, there is and there will be a decreasing trend in the contribution of fossil fuels, which includes coal and natural gas, and it is projected to decline to 31% by the year 2050. In particular, by 2050, solar and

wind energy will play a significant role, contributing to approximately 48% of the energy generation mix [5]. So, the energy transition process will require much more efforts in the next future for reaching the goal defined by the European Green Deal. Nevertheless, the main renewable energy plants (hydropower plants, wind turbines, solar panels, etc.) are instable and not always available because of oscillations in energy availability along their cycles (seasonality, day, night) and peaks in the demand. To overcome this issue, the excess of energy generated in periods of low demand could be stored and suddenly used in case of necessity. This kind of energy storage is represented by batteries [6]. The use of batteries has a key role for energy transition because it represents the connecting link between the reduction of fossil fuels consumption and promotion of renewable energy resources. According to Baur et al., “International Energy Agency estimates that limiting temperature increase to below 2°C as set out by the Paris Agreement would require energy storage capacity to triple by 2050”. The bottom graph shows the projections of energy storage installations in GW and It’s possible to see that by 2040 (building upon a base of 9 GW/17 GWh deployed as of 2018), the market will increase to 1095 GW/2850 GWh. This represents a remarkable more than 120-fold increase [5].

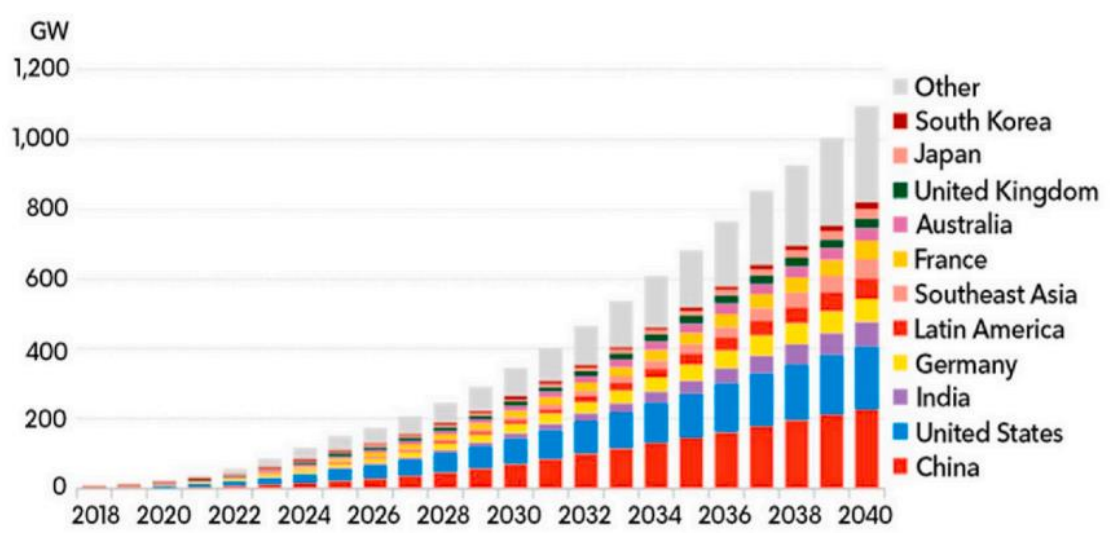


Figure 2 - Prediction of global energy storage installation by 2040 [5]

1.2. Stationary batteries and goal of this thesis

Stationary batteries, often called stationary storage batteries, are devices designed to store and release electrical energy on a continuous or scheduled basis. Unlike batteries used in vehicles, stationary batteries are designed for long-term applications and are usually installed in a fixed location, such as power generation plants, electricity distribution grids, or storage systems for homes and companies. The reasons why stationary batteries are so important and widely used today are due to their countless qualities:

- They have several applications, mainly for storing the energy from renewable sources and using when there is no sunlight or wind (in case of solar panels or wind turbines);
- They contribute to keep electricity grids stable by reducing peak energy demand during times of high loads;
- They represent a reserve energy; in fact, they provide power to ensure the operation of critical systems during interruptions (e.g. blackout) and can help to balance the power grid, adjusting the energy supply as needed;
- Finally, stationary batteries contribute to reduce electricity costs by storing energy during periods when it is cheaper and releasing it when prices are higher.

Nevertheless, there is the necessity to evaluate the environmental impact of each kind of stationary battery, because there are some critical issues that must be addressed (materials used, energy for construction and derived impact on the environment). These aspects will be discussed more in detail in next chapters. In particular, this thesis focuses on Vanadium redox batteries, which are analyzed through the methodology of Life Cycle Assessment (LCA). This thesis firstly contributes to define an overview of the state-of-the-art on the environmental studies on redox batteries, and, more specifically, on Vanadium redox batteries. Basing on this knowledge, this study aims to gather the best available inventory data to perform a LCA study on this type of battery and to identify the main gaps and limits that should be addressed in future works to enhance the robustness of the LCA calculations. Preliminary impact results are provided as well.

2. Technology of batteries

2.1. Electrochemical energy storage: how it works and which types exist

An important kind of battery that nowadays is assuming a relevant role in energy field is the electrochemical energy storage. This system transforms chemical energy into electrical energy through a redox reaction. In this process, the chemical substance loses electrons during oxidation, while it gains electrons during reduction. The oxidizing agent undergoes reduction to gain electrons, while the reducing agent gets oxidized and releases electrons. The fundamental components of any electrochemical energy storage system consist of an anode, a current collector, an electrolyte, and a cathode. By connecting electrochemical cells in series or parallel, the battery's voltage and energy capacity are determined. The current flow is affected by the resistances of the entire circuit. Despite this kind of device represents an effective solution for storing energy there are some aspects that must be studied in depth, in particular the power and energy densities, the rate of charge/discharge and the safety. "Electrochemical energy storage can further be classified as: standard battery (lead acid, Ni-Cd), modern battery (Li-ion, Li-polymer, Ni-MH), special battery (Ag-Zn, Ni-H₂), flow battery (Br₂-Zn, vanadium redox), and high-temperature battery". (Folorunso et al., 2023).

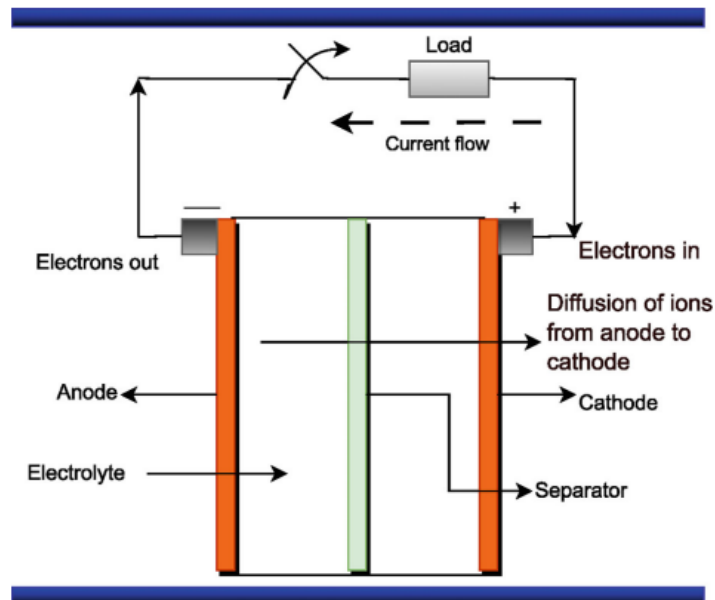


Figure 3 - Battery elements in an electrochemical storage system [8]

Currently, there are different chemical elements used as anode and cathode, and each of them has pros and cons that define the battery structural type. The following are the most common electrochemical batteries:

- Lead acid batteries, are the oldest electrochemical batteries. The anode is composed of lead, the cathode of lead dioxide, and the electrolyte is sulfuric acid, involving internal cell reactions. This type of battery is cost-effective and offers a long lifetime. However, it is composed of heavy components, which restrict its application to limited uses. They excel in terms of charge retention, scalability and recyclability. Nonetheless, they suffer from drawbacks such as low energy density and environmental hazards (e.g. acid leakage), scarce performance, limited temperature stability and corrosion;

- Nickel batteries, that present different structural types, but the nickel-cadmium (Ni-Cd) is the most common employed. The anode is nickel hydroxide, the cathode is cadmium and alkaline is used as the electrolyte. The structural design for nickel batteries remains consistent, with distinctions primarily arising from their electrode configurations. Nickel-cadmium batteries are particularly expensive for their high efficiency, it has a quite high toxicity and low energy density;
- Sodium sulfur batteries, where the sodium is the anode, the sulfur is the cathode and sodium-beta-alumina is the electrolyte. Sodium-sulfur batteries are subjected by sodium-polysulfide migration, formation of dendrites, limited discharge capacity, undesirable cycling behavior, and loss of sodium when reacting with electrolytes. Despite these drawbacks, sodium-sulfur batteries offer advantages such as high energy and power density, cost-effectiveness and a long lifetime;
- Lithium-ion batteries, that are at present the leading technology for electrochemical energy storage. Essentially, these batteries are characterized by anodes composed of carbonaceous and conductive polymer materials, while the cathode materials can include lithium-cobalt-oxide, lithium-iron-manganese-oxide or lithium-iron-phosphate. Various lithium alloys could be used as electrolyte. A separator is employed to isolate the active materials from the anode, typically consisting of porous materials that facilitate ionic conduction between the electrode and electrolyte.

However, it's important to note that the economic considerations related to lithium production and the scarcity of this mineral pose challenges for its application in grid power energy generation. Lithium-ion batteries presents some key issues, including low energy density, high costs of active materials, low voltage, power loss, a significant increase in resistance and a sensitive response to external factors [8].

2.2. Redox batteries for stationary applications

Next to the common batteries briefly described above, redox batteries (also called flow batteries) are alternative electrochemical energy storage devices playing an important role in stationary energy storage application (Kebede et al., 2022). Vanadium, polysulfide-bromide, iron-chromium, cerium-zinc, and zinc-bromine are all examples of redox batteries. Unlike conventional batteries, in redox battery technology the energy is not stored within the electrodes but in electrolytes in two separate external tanks. Redox batteries are able to store energy in significant quantities and distribute this energy across various entities. This technology is primarily designed for large-scale stationary applications that require several kilowatts of power.

One of the notable advantages of redox batteries lies in their ability to control power and energy densities, making them well-suited for applications in power systems such as power quality regulation, load balancing, and green energy storage. In Figure 4, a simplified illustration of a redox battery is provided, depicting key components like the ion exchange membrane, the electrolyte tanks (anolyte and catholyte), the electrodes and the load or power source used to recharge the battery when reactants are depleted.

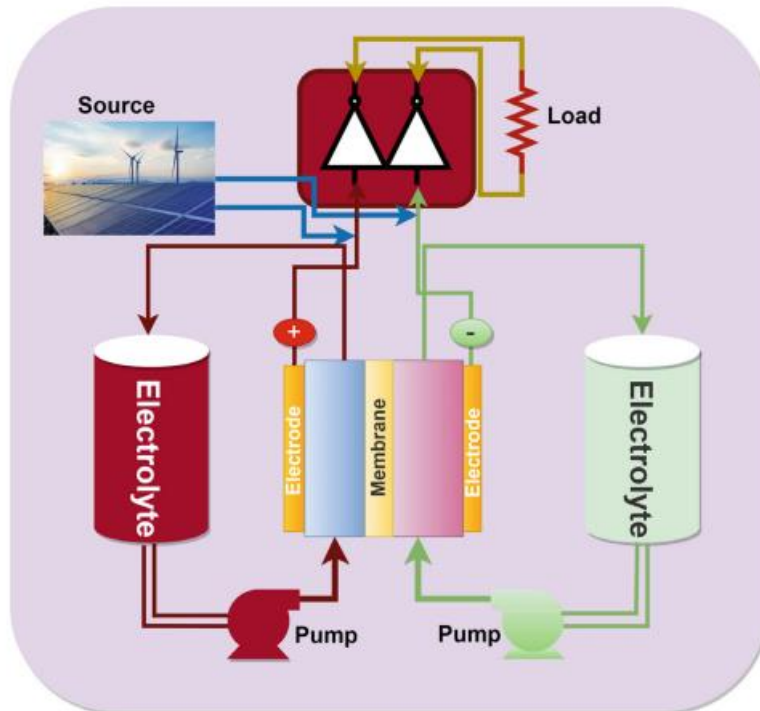


Figure 4 - Typical configuration of a redox battery [8]

The membrane, particularly in vanadium flow batteries, plays a critical role in the overall battery system. The quality and affordability of redox or flow battery membranes are crucial factors determining the battery's cyclic performance and economic viability. Ideal flow battery membranes should exhibit excellent chemical stability, ionic exchange capacity and conductivity, while also being cost-effective to produce.

Redox batteries present also some issues such as high ohmic resistance in graphite anodes, the high cost of active materials and nowadays limited application to stationary use [8]. However, these kinds of batteries have all the features to be globally employed in the next future because of their broad lifetime, easy scalability and low conservation prices [9]. Nowadays, due to the need of employing ever greener technologies, is essentially to evaluate the environmental footprint of different batteries, in order to choose which is the best solution.

2.3. Vanadium redox flow batteries

Between the different redox batteries, “the VRFB (vanadium redox flow batteries) are considered to be the closest to reach a commercial success” [10]. In a VRFB, electrical energy is generated through the electrochemical redox reaction involving vanadium ions with four potential oxidation states. These ions are dissolved in an electrolyte. The system is composed by a negative side, where the electrolyte (anolyte) contains V^{2+} and V^{3+} , and a positive side, where the electrolyte (catholyte) contains V^{4+} and V^{5+} (the latter in the form of oxides VO^{2+} and VO_2^+ , respectively) [10]. Typically, a VRFB system comprises at least three important components and materials:

- The electrolyte, that represents the most employed active material in the vanadium redox flow battery system, since it stores energy in chemical forms [11]. It enhances the solubility

of vanadium species and provides protons necessary for conducting electric current in the cells and balancing the primary reactions of the battery [10]. The energy capacity depends by its concentration. Usually, the electrolyte is composed of vanadium in different oxidation states and supporting additives like sulphuric and hydrochloric acids. The supporting electrolytes serve the purpose of enhancing the conductivity of the primary electrolyte and facilitating the transfer of hydrogen ions during the positive half-cell reaction. Unfortunately, conventional supporting additives have low solubility and stability so it decreases the energy density of VRFB. Several research reported that by using organic additives there could be an increase thermal stability of electrolytes;

- The electrodes, in which they play a passive role in the electrochemical reaction, serving as a surface for the reaction to take place. Hence, for optimal electrochemical reactions on the electrode area, specific electrode characteristics are essential. These include a large surface area, a wide electrochemical window, high conductivity, electrochemical reactivity, chemical stability and cost-effectiveness. Experimental findings indicate that carbon-based materials, including carbon felts, carbon paper, carbon nanotubes, graphite felts, and graphene, are highly suitable owing to their excellent electrical conductivity, substantial specific surface area and cost-effectiveness. To minimize the ohmic voltage loss resulting from internal resistance in VRFB, porous electrode structures have been employed. As the ohmic voltage loss intensifies with increased operating current, especially in large-scale VRFB applications, efforts have been made to decrease electrode thickness as a strategy to mitigate ohmic loss. However, it's crucial to note that reducing electrode thickness also decreases surface area, potentially causing concentration and electrochemical polarization. Consequently, the optimal electrode thickness must be carefully chosen to obtain optimal performance and efficiency;
- The membrane, which plays a crucial role in influencing the battery's performance. Its primary functions include isolating the positive half-cell from the negative half-cell to prevent the unwanted movement of electrolytes and completing the electrical circuit by facilitating the transport of protons. An ideal membrane is characterized by low permeability to minimize the self-discharge rate, high ion conductivity to reduce ohmic loss during proton transport and cost-effectiveness. To mitigate cross-contamination, a primary factor contributing to the degradation of performance in VRFB, it is crucial to study the ion transport mechanism for optimizing the VRFB's overall performance. Nafion is the most employed as the membrane material in VRFB due to its excellent conductivity and favorable chemical stability. Nevertheless, its high permeability and cost make it unsuitable for large-scale applications [11].

Other secondary but fundamental components that characterize VRFB are a pair of tanks for storing both electrolytes, an electrochemical stack that generate electric power and a hydraulic subsystem managing the flow of electrolytes between the aforementioned components.

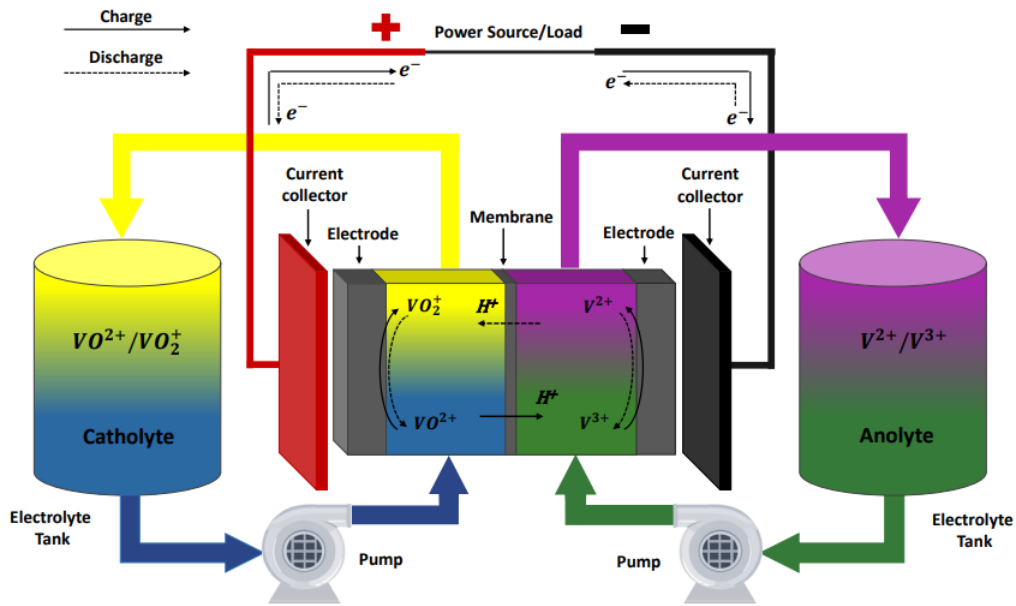
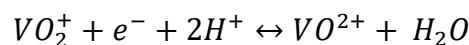


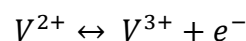
Figure 5 - Scheme of a VRFB and reactions involved [10]

When the battery is working, the electrolytes are transported from the tanks to the electrochemical stack, where the electron transfer reaction occurs and this reaction takes place at the electrode surfaces. Inside the stack, a proton exchange membrane keeps the two electrolytes separated, allowing the passage of protons to close the internal circuit and maintain the electrical neutrality of the solutions. Once the electrolytes complete the circuit within the stack, they return to their corresponding tanks. It is common to arrange multiple cells in series to form a stack, with the aim of achieving higher voltages and power. In this configuration, each cell is separated by a bipolar plate, which not only provides structural support to the stack but also serves as an electrical connection between adjacent cells. The electrons released in the electrochemical reaction are accumulated by the current collectors placed at the end cells of the stack, connecting to the power load/source. The battery's working principle is reversible, so when there is an external voltage, the process takes place in the opposite direction, regenerating the reactants used during discharge. In addition, the energy stored in the system is linked to the volume of electrolyte in the tanks and the concentration of vanadium charges (V^{2+} and V^{5+}). Naturally, concentrations of charged species rise during the charging process and decline during discharge. Due to constraints in vanadium solubility, the overall vanadium concentration in each electrolyte typically remains below 2 M [10].

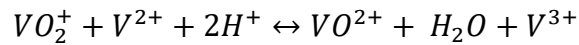
In the electrochemical discharge process, the positive half-cell experiences a reduction reaction, specifically involving the acquisition of an electron on the anode's surface, as indicated by:



In the negative half-cell an oxidation reaction takes place, involving the loss of an electron on the cathode's surface, converting V^{2+} ions to V^{3+} ions. This electrochemical process can be formulated as:



Generally, the overall reaction can be written as:



Where \leftrightarrow indicates a reversible process [11].

Unfortunately, in VRFB, there are additional undesirable reactions occurring at a slower rate that can significantly impact the system's performance. These processes are usually due to imperfections in the membrane, allowing the passage of small amounts of water and vanadium, or to side reactions, so reactions occurring simultaneously with the primary reaction but to a lesser extent. Example of these side reactions are:

- Vanadium ion crossover beyond membrane;
- Water transfer from one half cell to another;
- Gas evolution side reactions, where the support electrolyte, presumed to be inert (such as water and protons) become involved in the electron transfer reactions, producing gaseous products;
- Air oxidation, when the oxygen present in the air dissolves in the liquid and contribute to the oxidation of V^{2+} to V^{3+} . This is due to the exposition of negative electrolyte tank to the atmosphere;
- Vanadium precipitation, caused by an overcoming of the concentrated solution over a certain threshold or by a thermal instability.
- Solid components corrosion, due to the acidic behavior of the electrolyte and the level of oxidation of VO_2^+ [10].

Despite these disadvantages, VRFB are considered as one of the best batteries for stationary applications since they present an high modularity, limited cross-contamination issues and an extended system lifespan of up to two decades. They exhibit a prolonged charge-discharge cycle, no dependence from power and energy, low storage losses and so significant efficiencies until 80%. Another advantage is indicated by their flexibility, since the storage of electrolytes is due to the battery stacks, allowing easy adjustments in energy storage capacity by adding or removing electrolytes as needed. After the utilization phase, air oxidation or ion imbalance contribute to capacity loss of vanadium electrolytes but it can be restored through a simple remixing of the two half-cell solutions, facilitating electrolyte reuse. Additionally, depending on the battery design, straightforward decommissioning processes can be implemented to separate various components and materials for recycling purposes [1].

2.4. Optimization of VRFB over the years

In the last years, many researchers have developed new improvements in order to increase performances and reliability of the battery. The electrode plays a key role in assessing the performance of the battery. In their study, Mayrhuber et al. designed carbon paper electrodes with laser perforations to increase electrolyte accessibility and enhance overall battery performance. Kumar et al. explored the efficiencies and pressure drop in a VRFB, comparing interdigitated and serpentine flow fields. The battery featuring a serpentine flow field demonstrated a higher energy efficiency and minimal pressure drop.

In 2018 and 2019, Yaji et al. have employed topology optimization to enhance flow field design and subsequently improve battery performance. They framed the flow field design as a maximization problem for the generation rate of vanadium ions, incorporating a characteristic porous model. They introduced a mass transfer coefficient coupled with local velocity to examine how the design depends on porosity and pressure loss. [15] also showed computational design based on topology optimization to automatically generate an optimized 3D flow field design for VRFB, resulting in enhanced performance. Both studies concluded that the interdigitated flow field proves to be optimal.

Over the flow field considerations, operating conditions play a crucial role in flow battery performance, including factors such as temperature and flow rate [16], [17]. Ma et al. observed that increasing the flow rate leads to higher battery capacity but reduces system efficiency. They implemented strategies to optimize the system under varying flow rates. Zhang et al. discovered that elevated operating temperatures result in increased peak discharge power density, but at the cost of capacity decay and reduced coulombic efficiency.

In addition, electrodes largely influence all voltage losses. In their study, Kim et al. developed a carbon felt with an activity gradient in the in-plane direction. This design aimed to achieve uniform reaction rates, enhance electrolyte utilization and ultimately improve energy efficiency. The optimization efforts focused on flow-through batteries but did not take into account the impact of the flow field. When incorporating a flow field, the battery can use thinner electrodes to reduce ohmic loss, leading to improved cell performance, including enhancements in limiting current density and peak power density.

Simultaneously, numerical simulation plays a crucial role in fine-tuning the design of flow batteries. In their work, Jiang et al. created a gradient porous electrode in the through-plane direction. They observed that this design resulted in the uniformization of local reaction current density and an increase in overall capacity. Tsushima et al., on the other hand, developed a 2D model to investigate the impact of electrode properties and channel geometry on battery performance. Their study involved a multi-parameter optimization approach to enhance the design of VRFB [21].

In 2021, with the growing interest in large scale VRFB, He et al. studied and tried to optimize the design of the gradient electrode, the specific surface area, porosity and various flow fields. They found that in a large scale VRFB system, maintaining a high porosity proves effective in minimizing concentration polarization. This not only improve battery performance but also decreases pressure loss. To enhance mass transfer even more, larger diameter fibers can be employed and the electrode's specific surface area can be increased by modifying the fiber's surface [21].

Another important element in every VRFB system is the membrane. In addition to the environmental impacts associated with its production and the expenses involved, it serves as a primary factor influencing costs [22]. Nafion, a sulfonated fluorocarbon polymer, is the most frequent employed as membrane material in flow batteries, but there have been advancements in the development of several alternative materials for battery applications. Recently created membrane materials demonstrate enhanced ion conductivity and stability and have undergone testing to potentially enhance battery performance. However, comprehensive impact assessments are hindered by incomplete production data. Nafion remains the predominant membrane material in VRFB at present [23]. Among the numerous options for membrane materials in VRFB, sulfonated polyether ether ketone (sPEEK) stands out as a highly promising alternative to the widely used Nafion. Substituting Nafion with sPEEK as the membrane material results in a reduction of environmental impacts across all evaluated categories. Nevertheless, it is essential to consider significant constraints and uncertainties inherent in this analysis. Initially, the energy consumption related to the production of the sPEEK membrane is calculated exclusively based on the shaping and polycondensation process stages. Owing to insufficient data, other process steps are omitted, likely resulting in an underestimation of the overall energy demand [22].

3. Life Cycle Assessment (LCA)

3.1. LCA methodology

It is essential to adopt a holistic view of the battery life cycle [11]. Life Cycle Assessment (LCA) is a structured and uniform approach that collects data on energy and material used throughout a product or system's life cycle, for example from resource extraction to product disposal. It is used to assess and examine its possible environmental impacts in line with the study's goals [1]. The life cycle assessment is one of the most established and universally recognized tools to calculate environmental impacts throughout the life cycle of products or services (Product Environmental Footprint-PEF). According to the standard ISO 14040-44 (defined by International Standard Organization [25], [26]) and with the support of the International Reference Life Cycle Data System (ILCD) handbook [27], the life cycle assessment is characterized by four main steps:

- Goal and scope definition, in which several methodological choices are taken, such as defining system boundaries, the object of evaluation, the functional unit, collecting life cycle inventory data and requirements, and establishing the foundation for impact assessment (impact categories and life cycle impact assessment methods). The system boundaries differentiate the studied product system. The life cycle analysis could be developed using different system boundaries, such as the so-called cradle-to-gate and cradle-to-grave [11]. Cradle-to-gate refers to the phases involving the acquisition of raw materials up to the assembly of the product, just before it is transported to the end user. On the other hand, cradle-to-grave boundaries encompass the product's utilization and its phases at the end of its life, providing a comprehensive view of its entire life cycle [12]. Nowadays this last term is questioned because there is the need to adopt a circular approach, where part of the material is reinserted into a new production cycle. This is the base of the so-called cradle-to-cradle approach.
- Life cycle inventory (LCI), that involves the compilation and quantification of all the inputs (materials, energy, etc.) and outputs (emissions, waste, etc.) associated with a product or system throughout its life cycle. Essentially, it's a comprehensive inventory of the environmental and resource-related aspects of the product or system. The LCI data collected in this phase forms the foundation for the subsequent phases of LCA. It allows for a detailed analysis of the resource usage and environmental emissions associated with a product, from its raw material extraction to its disposal or end-of-life management.
- Life cycle impact assessment (LCIA), where the potential impacts on the environment of the analyzed product or service are quantified and evaluated. There is a wide range of available methods and impact categories, even though the most frequently requested is the assessment on climate change indicator. In general, the LCIA is summarized into two mandatory sub-actions (classification and characterization) and two optional ones (normalization and weighting, that make comparison of the processes and materials easier). The classification identifies the resource and emission flows (resulting from the inventory) that contribute to the impact for a specific indicator; characterization is the quantification of specific environmental impacts of the different resource and emission flows.
- Interpretation of the results, it represents the last phase, where all the results are discussed and interpreted, verifying whether targets have been met [11].

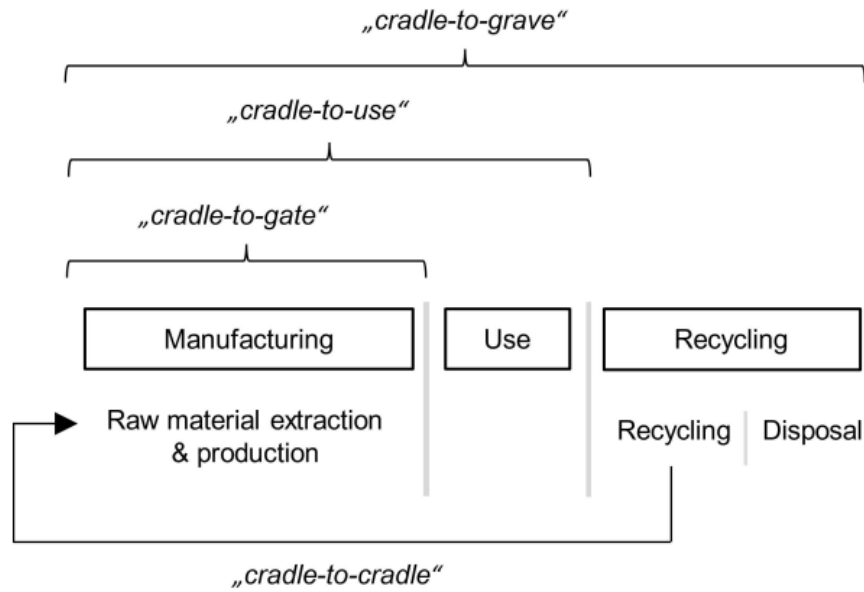


Figure 6 – Different system boundaries in a LCA of a product [11]

3.2 LCA of batteries in the European framework

In the actual context, European Commission developed the Product Environmental Footprint Category Rules (PEFCR) that provides specific rules for calculating the environmental impact of a product throughout its life cycle, from raw material extraction to production, distribution, use and disposal. In addition, by establishing consistent rules and criteria, PEFCR enables companies to measure and compare the environmental footprint of their products accurately. This allows for informed decision-making to reduce environmental impacts and improve sustainability across various industries.

In July 2023, the European Parliament endorsed a new regulatory framework [29] aimed at guaranteeing a secure, circular, and environmentally sustainable value chain for every battery sold or used within the European Union, ensuring their safe and sustainable management from production to disposal. Sustainability standards comprises regulations about carbon footprint, minimum recycled material thresholds, performance benchmarks, battery durability criteria and guidelines on end-of-life of battery. The majority of these measures will come into force by 2024, avoiding the necessity for transposition into national legislations. This framework applies to all economic actors, including suppliers, manufacturers and distributors, ensuring their compliance with the law's obligations.

Originally introduced by the European Commission in 2020 as a replacement for the 2006 batteries directive, the new EU battery regulation requires that all batteries distributed or employed within the EU adhere to specified sustainability standards. The key dispositions comprise:

- Limitations on the employment of harmful substances, specifically cadmium, lead and mercury;
- Implementation of regulations concerning carbon footprint (CF), such as the compulsory CF statement by 2025, CF categories by 2026 and the setting of minimum CF thresholds by 2028;

- Criteria for the use of recycled content;
- Imposition of extended producer responsibility to oversee the collection and handling of batteries;
- Setting a target for portable batteries to achieve a collection rate of 45% by 2023, growing to 73% by 2030;
- Implementation of rules for battery recycling, including targets of 75% for lead-acid batteries, 65% for lithium-based batteries, 80% for nickel-cadmium batteries and 50% for other waste batteries, to be achieved by 2025;
- Introduction of material recovery objectives, aiming for 90% recovery rates for cobalt, nickel, copper, and lead by 2027, increasing to 95% by 2031 and 50% recovery for lithium by 2027, until 80% by 2031 [30].

Another important point regarding the LCA regulations is the battery passport, that represents a digital product passport. The purpose of the battery passport is to improve transparency throughout supply and value chains for all involved stakeholders, facilitate the sharing of information and provide details on carbon footprint of their production processes, know the source of materials employed and recycled materials. It must be completely compatible with other digital product passports outlined in the Eco-design standard concerning the technical aspects of end-to-end communication and data transmission. On the other hand, the regulation addresses certain concerns regarding the sensitive information requested by the battery passport. Specifically, it is established that certain necessary sensitive information should not be publicly accessible. The adopted document points out that this restriction applies to information related to dismantling, including safety measures and detailed battery composition data, which are crucial for repairers, remanufacturers, second-life operators and recyclers. Additionally, the battery passport include among others, the following useful data:

- The composition of the battery;
- Information about CF;
- Details regarding responsible provisioning practices;
- Recycled content;
- Renewable content share;
- Nominal capacity, minimal, nominal and maximum voltage, with temperature ranges when necessary;
- Battery lifetime expected;
- The energy efficiency during the first round trip and when the battery is at 50% of its cycle-life;
- The resistance within the battery cells and packs;
- EU declaration of conformity [31].

4. State of art on LCA of Vanadium redox flow batteries

Research on the environmental effects of redox flow battery technologies appears to be not wide, but even not particularly scarce. 23 studies addressing this subject were found. This limited number of studies can be attributed to the relatively recent status of flow batteries in the battery technology landscape. The majority of Life Cycle Assessment studies on flow batteries emerged post-2015, with a clear increase in publications from 2020 onward. The predominant focus in these studies is on vanadium-based flow battery systems (22 studies), reflecting their commercial availability. In particular, the first environmental assessment of VRFB was carried out in 1999 and there were no further scientific publications on this topic until 2015.

Researchers emphasize the significance of primary data, which unfortunately is scarce and unreliable at various stages of Life Cycle Assessment (LCA) studies. For this reason, in almost cases, papers focus on secondary data, so by taking information from past scientific literature (publications) and sometimes were obtained by experiments ([32]) or manufacturers' data ([33], [34], [1], [23]). Using secondary data is a commonly employed method in academic literature and this approach is relatively easy and fast for its expediency, reliability and uniformity, given that the data originates from a certain source.

Furthermore, the researchers encounter challenges in obtaining consistent data, primarily attributed to the diverse sources of the studies. Almost all the studies were conducted by using Ecoinvent as background data source [24], except for the first study (Rydh), which took all the data from past research, manufacturer and supplier from Sweden, while AlShafi with Bicer and Shittu et al. have used the database GaBi. The GaBi software is employed for conducting analyses and offers a continually updated and readily accessible database for systems or products. Additionally, it takes into account the environmental impact, offering alternative choices for distribution, manufacturing, pollution, sustainability, and more. This software aids businesses in achieving optimal product sustainability performance by employing life cycle assessments with the latest and most precise databases. However, the main limitation of GaBi is lack of certain data [36]. Blume et al., besides Ecoinvent, made use of Umberto LCA+ as database. Concerning the software employed for life cycle assessment in the course of publications, the most used was SimaPro, while in the articles of Mostert et al. and Weber et al. the study was evaluated by OpenLCA.

4.1. System boundaries

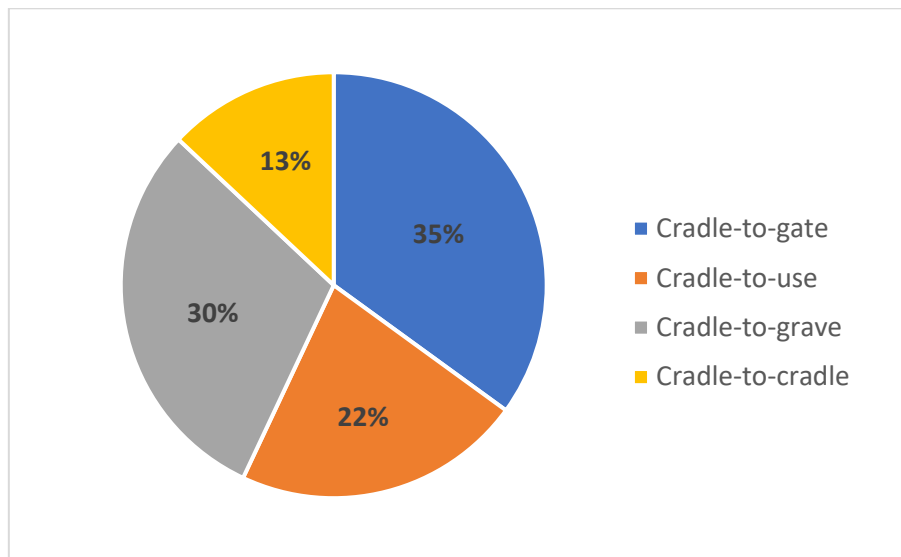


Figure 7 - System boundaries of VRFB studies

The pie chart shows the system boundaries distribution of all the scientific articles. Overall, the LCA on VRFB were conducted mainly using a cradle-to-gate (8 articles) and cradle-to-grave (7 articles) analysis. In particular, Rydh, Unterreiner et al. and Weber et al. have used a cradle-to-cradle approach, so by evaluating directly the option of recycling the components of vanadium flow batteries. However, many others publications have dealt with the subject of recycling and reuse but with some approximations. Another kind of system boundary, but less known, is cradle-to-use approach, so by analyzing phases involving the acquisition of raw materials up to the utilization of the battery. It is the case of Hiremath et al., Mostert et al., Stougie et al., Baumann et al. and AlShafi with Bicer.

4.2. Functional unit and source of data

The functional unit (FU) is the unit to which the final impacts are ascribed. It represents the measured function or service offered by the product or system. This unit enables the comparison of various products or systems by assessing their environmental impact per unit of function. In many studies (10 articles) the functional unit was set to 1 kWh, while in 6 publications is used 1 MWh. All the remaining articles used other functional units.

As said before, some studies take battery technical specifications and/or inventory data from past scientific publications. In particular, Rydh's data are taken as reference for Hiremath et al., Weber et al. and Mostert et al.. Consequently, characteristics of battery and life cycle inventory from Weber et al., were used by many subsequent researchers.

In the upcoming sections, the literature review undertaken for this study will be examined by dissecting each life cycle phase individually. This approach aims to partition information related to each specific stage, facilitating a comparison of how various papers handle the same phase with variations in assumptions.

4.3. Phases of Vanadium batteries life cycle

4.3.1. Material extraction

It involves the extraction of raw materials that will undergo subsequent processing and utilization in the manufacturing phase.

Vanadium finds its primary application in metallurgy, serving as an alloying agent for iron and steel. This particular usage is reported to constitute approximately 94% of the vanadium consumed domestically in the year 2021. Regarding the remaining portion of vanadium consumption outside metallurgy, it is predominantly employed as a catalyst in the production of maleic anhydride and sulfuric acid. This leaves minimal space for the utilization of vanadium as electrolyte in battery systems. According to recent data, China is the country that owns the largest vanadium reserves, following Russia, South Africa and Brazil [43]. Some studies don't specify the origin of vanadium, but overall the extraction considered is located in South Africa and for some studies in China ([1], [6]).

Before advancing to the manufacturing and assembly phases, it is essential to highlight a specific discovery that concerns the differentiation between the material extraction and manufacturing phases. Although the literature often show this distinction with apparent clarity in data modeling, real-world scenarios prove otherwise. This discrepancy arises because, between these two stages, there exist additional phases of material processing and production. These stages are frequently considered either less pertinent to the study's objectives or excessively intricate for detailed analysis.

Some publications incorporate material processing within the material extraction phase [44], often labeling it as material production, while others incorporate these processes into the manufacturing stage [45].

The latter approach appears to be more commonly adopted in existing literature, possibly influenced by the tendency to associate the term "material extraction" more narrowly with mining activities. Nevertheless, achieving a definitive demarcation between the two phases is not always feasible. Consequently, a comprehensive understanding of the processes encompassed in each phase is imperative for accurately interpreting the life cycle impacts.

4.3.2. Manufacturing and assembly

The number of articles that focus on the manufacturing of VRFB is considerable and usually this phase was conducted within a single nation. The manufacturing phase is almost always coupled with the assembly one. It is useful to notice how the mentioned countries considered are quite homogeneous. Germany is one of the main countries in which VRFB production and assembly take place and for this reason it was used German electricity mix as reference for life cycle analysis ([40], [22], [1], [42]). In Silva Lima et al.'s article the VRFB is fabricated by Dalian Rongke Power Co. (China), while Weber et al. in the article took information on what the production process of vanadium is like from a mine operator in South Africa. The procedure involves the extraction of vanadium from titanomagnetite ores, which serve as the primary source of industrial V_2O_5 . In the initial stage, the ore undergoes processing to yield pig iron containing vanadium. This pig iron can be further treated in an electric arc furnace to produce steel and a byproduct in the form of vanadium-bearing slag during steel manufacturing. The slag, boasting an increased vanadium content of approximately 25%, is subjected to acid leaching processes for the extraction of vanadium pentoxide. This extraction process encompasses activities such as slag grinding, roasting and subsequent leaching

using ammonium sulfate and sulfuric acid. The resulting ammonium polyvanadate is then transformed into high-purity vanadium pentoxide through roasting, while any remaining slag is disposed of in landfills [22]. Vanadium pentoxide production site is assumed to be in South Africa for many studies [46], [22], [32]. In particular, Dassisti et al.'s study highlights three different techniques for preparing mixed acid vanadium electrolytes for VRFB in relation to their efficiency, suitability, and sustainability. The initial approach involves simply blending appropriate vanadium precursors to generate electrolyte. The second method is based on chemical reduction of V_2O_5 through oxalic acid. The third method, involves the electrochemical reduction of V_2O_5 using a self-constructed "H-shaped" electrolysis cell. Additionally, in two researches, the VRFB was assembled and tested in Italy [32], [46], in particular all the elements of the battery were sourced from southern Italy with the exception of the electrolyte synthesis reagents [32], [46] and vanadium pentoxide [14].

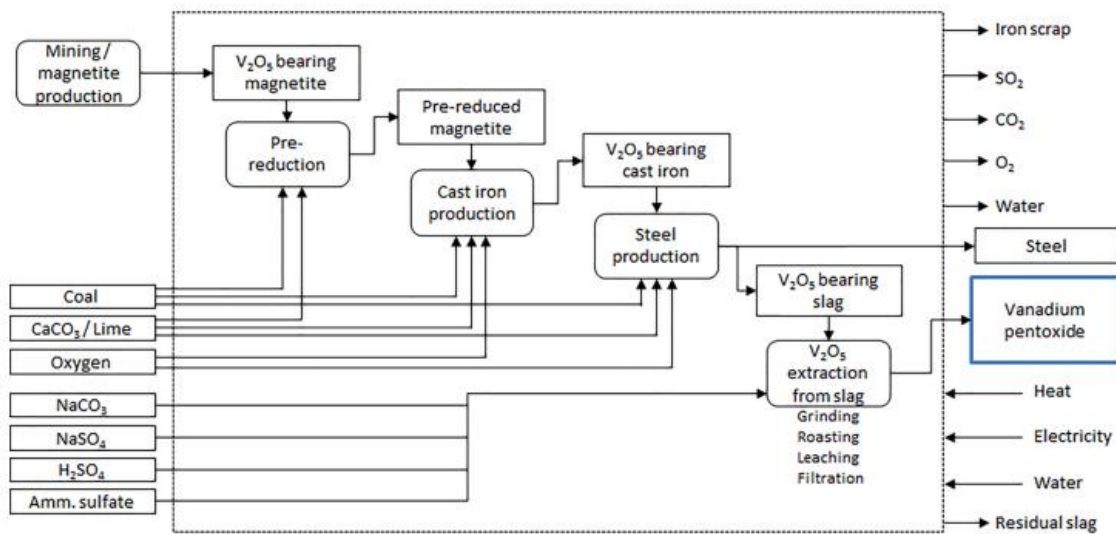


Figure 8 - Flowchart of the manufacturing of vanadium pentoxide [22]

4.3.3. Use phase

Previous literature has identified the utilization phase as a significant contributor to the overall impacts of battery-based storage systems in stationary applications [40]. The literature also provided recommendations for additional research in this area [6].

What Baumann et al. highlight as interesting is that, unlike various other battery varieties, the capacity of VRFB is dictated by the size of the tanks or the quantity and concentration of the electrolyte. Meanwhile, the power rating is influenced by the quantity of cells incorporated into a stack. Consequently, VRFB offer flexibility in design to accommodate the specific energy and power needs of a given application. The optimization of battery size results in a range of diverse battery configurations, depending on the particular application scenario.

The outcomes obtained from the analysis of VRFB exhibit a notable level of uncertainty. Nevertheless, VRFB demonstrate strong economic performance in scenarios where a higher energy-to-power (E/P) ratio is needed. This is applicable only in such cases due to the elevated cost associated with the separator membrane. Additionally, the findings regarding the carbon footprint are favorable for applications with high E/P ratios. Consequently, the performance of this battery

type varies significantly, depending on the characteristics of the specific applications under consideration. This variation also takes into account the trade-off between cost and CO₂ emissions.

4.3.4. End-of-Life and recycling

Examining the identified discrepancies in the literature review reveals an increasing on research articles that take into account the end of life phase. In fact, older publications are progressively centering their attention on the subject of recycling and reuse, reflecting an increased awareness of the environmental crisis but for these batteries is difficult to obtain detailed information about this step [33]. The primary objective of recycling is to reuse resources, thereby reducing the extraction of virgin material. The cradle-to-cradle approach serves as a model for this reuse, where recycled materials contribute positively during the initial material phase, as a form of credit.

Some studies have declared the absence in their articles of recycling option of the main battery components ([39], [33], [42], [48], [38]). da Silva Lima et al., made the assumption that 50% of electrolyte is recycled, while a few publications considered the recovery and recycling of metals ([49], [34], [48], [50]) and plastic ([49], [48]). Many earlier studies suggest, as a potential improvement for future research, the analysis of the impact of the recycling stage, highlighting an existing recognition of the scarcity of materials. In particular, Diaz-Ramirez et al. stated that recycling all the materials of VRFB can decrease the environmental impact by more than 50%.

If recycling process of all metals are taken into account (95% recycling) the end of life phase present a little influence on all impact categories. In some papers the losses occurring in the reprocessing and purification stages were considered in the end-of-life phase of the life cycle. Nevertheless, in the context of electrolyte recovery, these processes exhibit negligible environmental effects in terms of impact reduction compared to the impact reduction achieved by utilizing fewer new mineral resources for electrolyte production.

The comprehensive assessment of the end-of-life phase also relies on the transportation to the recycling or disposal site.

4.3.5. Transportation

The transport phase, which is usually analyzed, is difficult to find in literature due to insufficient data and uncertainties and for this reason in many articles is not taken into account ([33], [23]). For the scenario where no transportation is considered, the CO₂ footprint (associated with global warming) decreases by approximately 60% in the case of VRFB. Similarly, in terms of human toxicity impact, by excluding electrolyte transport in the study results in a reduction of around 27% [51]. L'Abbate et al. also takes into account the transport phase, but exclusively for the raw materials along with the packaging. Ultimately, the packaging was excluded from consideration as its impact on the overall life cycle was determined to be 0.05%. The transportation of reagents was determined based on the distance between the retailer and the location of electrolyte preparation. Gouveia et al. studied in a detailed way the weight of transportation in the LCA of VRFB, comparing different impact categories. The findings indicate that, within the climate change category, the primary contributors are the transportation of components and the battery structure (representing the cell stack components), with vanadium storage tanks following closely. This can be attributed to the shipment of essential electrolyte components from China and the electrolyte manufacturing taking place in Germany. The transportation to Portugal, where the battery is produced, holds significant potential for

consequences related to climate change, photochemical ozone formation, and acidification potential due to its substantial volume. Conversely, in the case of the ozone depletion category, the impact of transportation is minimal. Within the photochemical ozone formation category, the transport phase constitutes 53% of the overall impact, emerging as the most significant contributor. Among all the components assessed, transportation of vanadium electrolytes yield the most substantial potential consequences for acidification potential, contributing 38% to the total impacts [1].

In da Silva Lima et al. transportation encompasses the shipment of the complete battery unit from China to Belgium, including both the international and domestic transportation within Belgium. Transport plays a role in the overall impacts, due to the use of oil fuel in the shipping of the battery from China to Belgium.

In Diaz-Ramirez et al. transportation information derive from Weber et al. and Ecoinvent database. Specifically, it was assumed that the membranes and electrodes would be manufactured on-site, eliminating the need for transportation. Upstream processes of electrolyte production include not just the extraction of raw materials through mining but also involve the necessary transoceanic transportation of the electrolyte from South Africa to Europe. This transportation contributes significantly to the environmental footprint [50].

Overall, it is necessary to develop production site near to the assembly location in order to minimize the emissions.

4.4. Sensitivity analysis

VRFB inventory data are based on hypothetical information modelling the state of the art of VRFB. The inventory model incorporates data gathered from various sources, involving numerous assumptions and simplifications. Consequently, the resulting uncertainties are substantial, necessitating careful considerations during result interpretation [22]. For this reason many articles carried out a sensitivity analysis in order to check how the assumptions influence the study results [33], in this case to examine how alterations in the primary contributing processes, which exert the most significant impacts, might influence other alternatives. In this way, it aims to determine whether overall emissions could be enhanced as a result [36]. Some studies focus sensitivity analysis based on recycling and reuse scenarios ([39], [1], [48], [42], [6], [38]). In particular, Gouveia et al. conducted a scenario evaluation, where the electrolytes are made of 30, 70% or 100% of reused electrolyte. The capacity of the electrolyte can be regained by combining the solutions from the two half-cells and reinstating the balance of capacity. This process enables the electrolyte to be reused, potentially leading to a reduction in cradle-to-gate life cycle impacts [1]. On the other hand, Diaz-Ramirez et al. evaluated potential benefits of recycling scenarios for steel, copper, aluminum and plastic materials to the battery manufacturing stage. Another important scenario evaluation is based on energy source employed at the use phase. There were 5 articles that have analyzed this aspect ([22], [6], [36], [50], [40]).

For example, da Silva Lima et al. made a comparison between photovoltaic energy as a renewable source and wind energy. Across all impact categories, the environmental effects of electricity

generated from wind turbines are less significant than the impacts associated with photovoltaic systems [6].

| Authors | Title | Year | Ref. |
|----------------------------|--|-------------|-------------|
| Rydh | Environmental assessment of vanadium redox and lead-acid batteries for stationary energy storage | 1999 | [35] |
| Hiremath et al. | Comparative Life Cycle Assessment of Battery Storage Systems for Stationary Applications | 2015 | [40] |
| Sternberg et al. | Power-to-What? – Environmental assessment of energy storage systems | 2015 | [52] |
| Dassisti et al. | Sustainability of vanadium redox-flow batteries: Benchmarking electrolyte synthesis procedures | 2016 | [46] |
| Unterreiner et al. | Recycling of Battery Technologies – Ecological Impact Analysis Using Life Cycle Assessment (LCA) | 2016 | [39] |
| Weber et al. | Life Cycle Assessment of a Vanadium Redox Flow Battery | 2018 | [22] |
| Mostert et al. | Comparing Electrical Energy Storage Technologies Regarding Their Material and Carbon Footprint | 2018 | [33] |
| Stougie et al. | Multi-dimensional life cycle assessment of decentralized energy storage systems | 2019 | [41] |
| Jones et al. | Assessing the Climate Change Mitigation Potential of Stationary Energy Storage for Electricity Grid Services | 2019 | [49] |
| L'Abbate et al. | Small-Size Vanadium Redox Flow Batteries: An Environmental Sustainability Analysis by LCA | 2019 | [32] |
| Gouveia et al. | Life cycle assessment of a renewable energy generation system with a vanadium redox flow battery in a NZEB household | 2020 | [34] |
| Gouveia et al. | Life cycle assessment of a vanadium redox flow battery | 2020 | [1] |
| Fernandez Marchante et al. | Environmental and Preliminary Cost Assessments of Redox Flow Batteries for Renewable Energy Storage | 2020 | [51] |
| He et al. | Flow battery production: Materials selection and environmental impact | 2020 | [23] |
| Díaz-Ramírez et al. | Battery Manufacturing Resource Assessment to Minimise Component Production Environmental Impacts | 2020 | [48] |

| | | | |
|----------------------|---|------|------|
| Baumann et al. | Exploratory Multicriteria Decision Analysis of Utility-Scale Battery Storage Technologies for Multiple Grid Services Based on Life-Cycle Approaches | 2020 | [42] |
| Díaz-Ramírez et al. | Environmental Assessment of Electrochemical Energy Storage Device Manufacturing to Identify Drivers for Attaining Goals of Sustainable Materials 4.0 | 2020 | [53] |
| Da Silva Lima et al. | Life cycle assessment of lithium-ion batteries and vanadium redox flow batteries-based renewable energy storage systems | 2021 | [6] |
| Morales-Mora et al. | Life cycle assessment of a novel bipolar electro dialysis-based flow battery concept and its potential use to mitigate the intermittency of renewable energy generation | 2021 | [54] |
| AlShafi and Bicer | Life cycle assessment of compressed air, vanadium redox flow battery, and molten salt systems for renewable energy storage | 2021 | [36] |
| Shittu et al. | Life cycle assessment of soluble lead redox flow battery | 2022 | [37] |
| Díaz-Ramírez et al. | Acid/base flow battery environmental and economic performance based on its potential service to renewables support | 2022 | [50] |
| Blume et al. | Life cycle assessment of an industrial-scale vanadium flow battery | 2022 | [38] |

Table 1 - list of LCA studies on flow batteries

5. ENVIRONMENTAL LIFE CYCLE ASSESSMENT OF VRFB

5.1. Goal and scope

The main objective of this work is to evaluate the environmental impact of VRFB with a cradle-to-grave approach by analyzing the components and processes involved from the extraction of materials until their disposal and recycling. Exploring an extended cradle-to-cradle approach could be interesting; however, considering the relatively early stage of VRFB technology and its prolonged lifespan, assessing recycling possibilities or potential second-life options can only be considered from a future perspective [38]. The chosen functional unit for the life cycle is 1 MWh stored in the battery, since it is one of the most used in the past articles. The life cycle begins with the extraction of raw materials for the fabrication of individual battery components, the structure and other system elements. These raw materials are subsequently conveyed to industrial facilities for manufacturing. Following the production of each battery and system component, transportation is facilitated either by truck or sea vessel to Italy. In South Africa, the assembly of the VRFB prototype takes place, along with the overall assembly of the entire system [1]. The information regarding the life cycle inventory were taken from Weber et al. and da Silva Lima et al.. In particular, LCI of production phase were taken by the most complete and reliable data of Weber et al.. For this reason, this study was taken as reference for many other articles, such as Jones et al., Silva Lima et al., Blume et al. and Diaz-Ramirez et al.. Regarding manufacturing of fan and steel housing, final assembly, use and end of life phases the information derive from da Silva Lima et al., since it plays a more recent scenario of battery life cycle. The main difference is that in the following analysis production site takes place in South Africa, while in da Silva Lima et al.'s article China was the selected country. The database used is Ecoinvent 3.1.

5.2. Life cycle inventory (LCI)

The life cycle of VRFB is based on a renewable energy storage system, in particular for a photovoltaic plant. A diagram depicting the life cycle phases of the VRFB is presented in figure. It is assumed that the entire battery is manufactured in South Africa and then transported to Italy, where both the utilization phase and the end-of-life (EoL) activities take place.

The VRFB could be considered as a formation of three major components: the power subsystem, the energy subsystem and the periphery. The active area of the cells determines the power subsystem, whereas the electrolyte volume is associated with the energy subsystem. The remaining parts are designated as periphery [6].

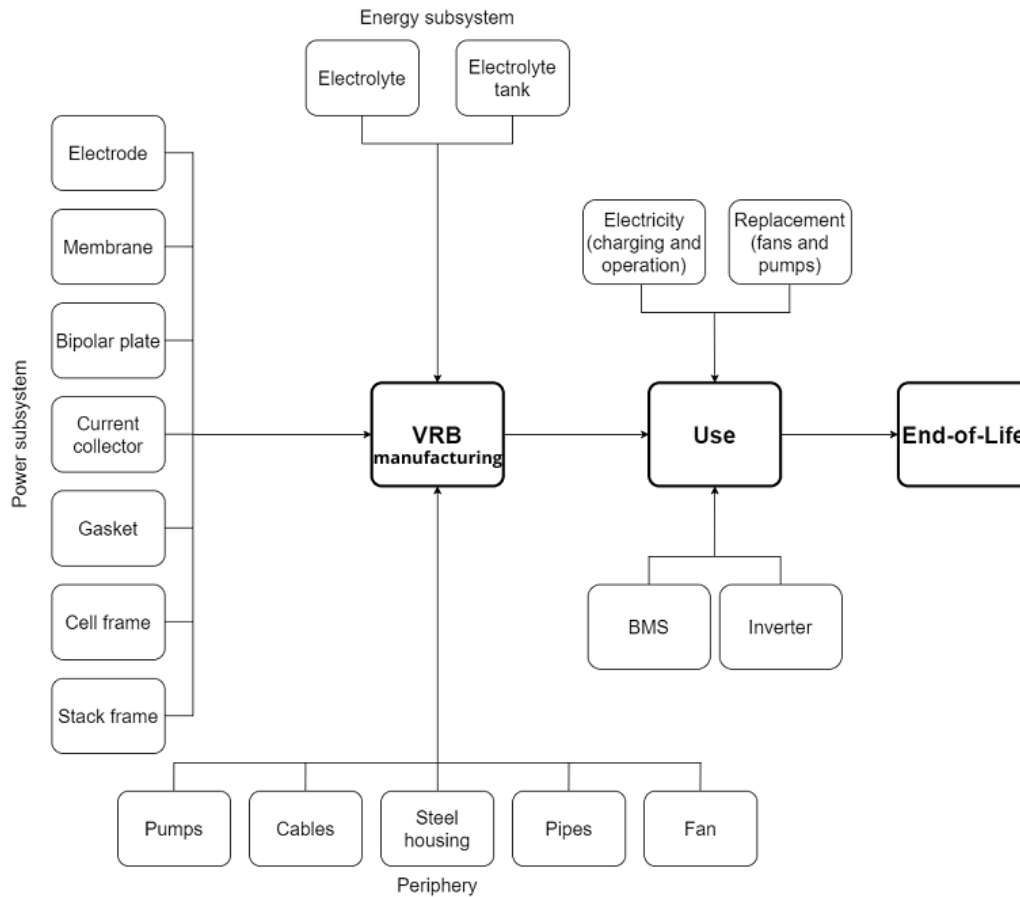


Figure 9 - Life cycle scheme of the vanadium redox flow battery. BMS is battery monitoring system [6].

5.2.1. Battery manufacturing (production phase)

Power subsystem

The power subsystem is comprised of a stack of cells, including membrane, electrodes, bipolar plate, current collector, cell frame, gasket, and stack frame. The stack frame serves to hold the cells together. The associated Life Cycle Inventory (LCI) is detailed in the following tables [6].

Nafion membrane

The investigated VRFB uses a Nafion ion exchange membrane known as the N-117 Nafion membrane, assumed to have a thickness of 183 μm . This specific type is frequently employed in VRFB systems. The production process for the membrane involves a polymerization reaction of tetrafluoroethylene (TFE) and a co-monomer [6]. It is assumed that the membrane is produced on site, avoiding extra transportation. The relevant Life Cycle Inventory (LCI) is outlined in the following tables [22].

| Flow | Amount | Unit |
|---|---------------------|---------|
| ⚙️ chemical factory, organics - GLO | 4*10 ⁻¹⁰ | Item(s) |
| ⚙️ heat, district or industrial, natural gas - Europe without Switzerland | 39.31000 | MJ |
| ⚙️ hexafluoroethane - GLO | 3.20000 | kg |
| ⚙️ soda ash, dense - GLO | 0.11000 | kg |
| ⚙️ sodium hydroxide, without water, in 50% solution state - GLO | 0.60000 | kg |
| ⚙️ sodium hypochlorite, without water, in 15% solution state - GLO | 3.00000 | kg |
| ⚙️ sulfur trioxide - GLO | 0.50000 | kg |
| ⚙️ tetrafluoroethylene - GLO | 1.30000 | kg |
| ⚙️ transport, freight train - Europe without Switzerland | 5.22000 | t*km |
| ⚙️ transport, freight, lorry, unspecified - GLO | 0.87000 | t*km |

Table 2 – LCI of Nafion membrane, input data

| Flow | Amount | Unit |
|---------------------------------|----------------|-----------|
| ⚙️ Membrane | 1.00000 | kg |
| ⚙️ bilge oil - RoW | 0.38000 | kg |
| ⚙️ sodium fluoride - GLO | 0.08480 | kg |
| ⚙️ spent solvent mixture - RoW | 2.81000 | kg |
| ⚙️ waste plastic, mixture - RoW | 0.11000 | kg |
| 🗑️ Carbon dioxide, fossil | 0.08880 | kg |
| 🗑️ Sodium chloride | 2.36000 | kg |
| 🗑️ Sodium hydroxide | 1.87000 | kg |

Table 3 – LCI of Nafion membrane, output data

Electrode

- Raw carbon felt made of PAN fibres

The chosen electrode is composed of carbon-based felts, and the fibers within these felts are derived from polyacrylonitrile (PAN). The initial carbon felt is created using acrylonitrile, primarily sourced from propene and ammonia through the Sohio process. The fiber manufacturing involves a polymerization process with methyl methacrylate, followed by fiber spinning to generate the PAN raw felt. Subsequently, the PAN raw felt undergoes thermal stabilization (oxidation) and carbonization. The usual carbon yield from a PAN-based precursor is around 50%, meaning that the production of 1 kg of carbon felt needs the use of 2 kg of PAN. To determine transport distances it is assumed that the electrode is manufactured on site, avoiding extra transportation [22].

| Flow | Amount | Unit |
|---|-------------|---------|
| ammonia, liquid - RoW | 0.91000 | kg |
| chemical factory, organics - GLO | 7.86000E-10 | Item(s) |
| core board - GLO | 0.01460 | kg |
| electricity, medium voltage - IT | 2.40000 | kWh |
| EUR-flat pallet - GLO | 0.00288 | Item(s) |
| heat, district or industrial, natural gas - Europe without Switzerland | 4.17000 | MJ |
| heat, district or industrial, other than natural gas - Europe without Switzerland | 2.08000 | MJ |
| heat, in chemical industry - RoW | 4.00000 | MJ |
| lubricating oil - GLO | 0.00022 | kg |
| methyl methacrylate - GLO | 0.10000 | kg |
| packaging box factory - GLO | 2.80000E-9 | Item(s) |
| particle board, for outdoor use - GLO | 4.30000E-5 | m3 |
| propylene - GLO | 2.24000 | kg |
| solid bleached board - GLO | 0.00196 | kg |
| steam, in chemical industry - UN-EUROPE | 0.12000 | kg |
| sulfuric acid - GLO | 0.03750 | kg |
| transport, freight train - Europe without Switzerland | 1.97000 | t*km |
| transport, freight, lorry 16-32 metric ton, EURO5 - GLO | 0.33000 | t*km |
| water, deionised, from tap water, at user - GLO | 4.25000 | kg |
| Water, cooling, unspecified natural origin | 0.12000 | m3 |

Table 4 – LCI of raw carbon felt made of PAN fibres, input data

| Flow | Amount | Unit |
|-------------------------------------|----------------|-----------|
| Raw carbon felt, PAN | 2.00000 | kg |
| Ammonia, IT | 0.00642 | kg |
| Ammonium, ion | 0.02570 | kg |
| BOD5 (Biological Oxygen Demand), NO | 0.07330 | kg |
| Carbon dioxide, fossil | 0.89000 | kg |
| COD, Chemical Oxygen Demand | 0.07330 | kg |
| DOC, Dissolved Organic Carbon | 0.02200 | kg |
| Propene | 6.19000E-5 | kg |
| Propene | 0.02480 | kg |
| Sulfate | 0.06970 | kg |
| TOC, Total Organic Carbon | 0.02200 | kg |
| Water | 23.50000 | kg |
| Water | 0.04050 | m3 |

Table 5 – LCI of raw carbon felt made of PAN fibres, output data

- PAN-based electrode

The following stages in PAN-based carbon felt production, namely oxidation and carbonization, are explicitly modeled and analyzed more closely due to the absence of appropriate reference processes in Ecoinvent. Mass balances are computed based on stoichiometry. Initially, the felt undergoes thermal treatment (oxidation), facilitating its stabilization. To compute transport distances it is assumed that the electrode is manufactured on site and, as a result, does not need transportation [22].

| Flow | Amount | Unit |
|---|---------|------|
| ⚙️ heat, district or industrial, natural gas - Europe without Switzerland | 0.87000 | 📦 MJ |
| ⚙️ heat, district or industrial, natural gas - Europe without Switzerland | 5.25000 | 📦 MJ |
| ⚙️ heat, district or industrial, natural gas - Europe without Switzerland | 0.07960 | 📦 MJ |
| ⚙️ Raw carbon felt, PAN | 2.00000 | 📦 kg |

Table 6 – LCI of PAN-based electrode, input data

| Flow | Amount | Unit |
|--------------------------|----------------|-------------|
| ⚙️ Electrode | 1.00000 | 📦 kg |
| ✅ Carbon dioxide, fossil | 1.31000 | 📦 kg |
| ✅ Nitrogen | 0.67000 | 📦 kg |
| ✅ Water | 0.66000 | 📦 kg |

Table 7 – LCI of PAN-based electrode, output data

Bipolar plate

The bipolar plate, a crucial component in VRFB, requires specific properties due to its numerous functions and the demanding operational environment. This research focuses on a composite material made by synthetic graphite and polypropylene as a binder, as these components prove particularly well-suited for redox flow batteries. The mass balance relies on a manufacturer's datasheet for bipolar plates. The production processes involve compounding and shaping. Compounding is executed on specialized extruders and typically includes metering, extrusion, and granulation steps. Precursor materials, synthetic graphite and polypropylene are sourced from Ecoinvent datasets, while adjustments are made to the data set for the extrusion process [22].

| Flow | Amount | Unit |
|--|------------|-----------|
| ⚙️ core board - GLO | 0.01460 | 📦 kg |
| ⚙️ electricity, medium voltage - IT | 1.32000 | 📦 kWh |
| ⚙️ EUR-flat pallet - GLO | 0.00288 | 📦 Item(s) |
| ⚙️ graphite, battery grade - GLO | 0.88000 | 📦 kg |
| ⚙️ heat, district or industrial, natural gas - Europe without Switzerland | 1.20000 | 📦 MJ |
| ⚙️ heat, district or industrial, other than natural gas - Europe without Switzerland | 0.42000 | 📦 MJ |
| ⚙️ lubricating oil - GLO | 0.00022 | 📦 kg |
| ⚙️ packaging box factory - GLO | 2.80000E-9 | 📦 Item(s) |
| ⚙️ particle board, for outdoor use - GLO | 4.30000E-5 | 📦 m3 |
| ⚙️ polypropylene, granulate - GLO | 0.14000 | 📦 kg |
| ⚙️ solid bleached board - GLO | 0.00196 | 📦 kg |
| ⚙️ steam, in chemical industry - UN-EUROPE | 0.12000 | 📦 kg |
| ⚙️ transport, freight train - Europe without Switzerland | 0.21000 | 📦 t*km |
| ⚙️ transport, freight, lorry 16-32 metric ton, EURO5 - GLO | 0.10000 | 📦 t*km |
| ⚙️ water, deionised, from tap water, at user - GLO | 0.08740 | 📦 kg |

Table 8 – LCI of bipolar plate, input data

| Flow | Amount | Unit |
|---------------------------------|----------------|-------------|
| ⚙️ Bipolar plate | 1.00000 | 📦 kg |
| ⚙️ waste plastic, mixture - GLO | 0.02500 | 📦 kg |

Table 9 – LCI of bipolar plate, output data

Current collector

It is assumed that the production of 1 kg of current collector needs 1 kg of copper. The processing method for the plate is considered to be sheet rolling. In line with this, the Ecoinvent dataset "sheet rolling, copper" is used [22].

| Flow | Amount | Unit |
|--|-------------|-----------|
| ⚙️ copper - GLO | 1.00000 | 📦 kg |
| ⚙️ metal working factory - GLO | 4.00000E-10 | 📦 Item(s) |
| ⚙️ sheet rolling, copper - GLO | 1.00000 | 📦 kg |
| ⚙️ transport, freight train - Europe without Switzerland | 0.20000 | 📦 t*km |
| ⚙️ transport, freight, lorry 16-32 metric ton, EURO5 - GLO | 0.10000 | 📦 t*km |

Table 10 – LCI of current collector, input data

| Flow | Amount | Unit |
|-----------------------------|----------------|-------------|
| ⚙️ Current collector | 1.00000 | 📦 kg |

Table 11 – LCI of current collector, output data

Cell frame

A polyvinylchloride (PVC) frame encloses each cell through an extrusion process. Consequently, the relevant Ecoinvent dataset for polyvinylchloride is employed, considering the extrusion method used in shaping the frame [22].

| Flow | Amount | Unit |
|--|---------|--------|
| ⚙️ extrusion, plastic pipes - GLO | 1.00000 | 📦 kg |
| ⚙️ polyvinylchloride, emulsion polymerised - GLO | 1.00000 | 📦 kg |
| ⚙️ transport, freight train - Europe without Switzerland | 0.20000 | 📦 t*km |
| ⚙️ transport, freight, lorry 16-32 metric ton, EURO5 - GLO | 0.10000 | 📦 t*km |

Table 12 – LCI of cell frame, input data

| Flow | Amount | Unit |
|----------------------|----------------|-------------|
| ⚙️ Cell frame | 1.00000 | 📦 kg |

Table 13 – LCI of cell frame, output data

Gaskets

Gaskets play a crucial role in connecting individual cells to prevent electrolyte leaks, necessitating resistance to acid corrosion. Various materials, namely FKM, EPDM and silicone, are available for gasket manufacturing. In this study FKM gaskets are employed. A notable type of FKM is the terpolymer comprising vinylidene fluoride (VDF), hexafluoropropylene (HFP) and tetrafluoroethylene (TFE). The forming process employs the reference process "extrusion, plastic pipes" [22].

| Flow | Amount | Unit |
|---|---------|------|
| extrusion, plastic pipes - GLO | 1.00000 | kg |
| hexafluoroethane - GLO | 0.33000 | kg |
| polyvinylfluoride - GLO | 0.33000 | kg |
| tetrafluoroethylene - GLO | 0.33000 | kg |
| transport, freight train - Europe without Switzerland | 0.20000 | t*km |
| transport, freight, lorry 16-32 metric ton, EURO5 - GLO | 0.10000 | t*km |

Table 14 – LCI of gaskets, input data

| Flow | Amount | Unit |
|---------------|----------------|-----------|
| Gasket | 1.00000 | kg |

Table 15 – LCI of gaskets, output data

Stack frame

The stack frame is a simple structure, consisting of two double steel T-profiles that keep the stack components together [6]. The size and weight are approximated using technical specifications from a representative steel profile datasheet [22].

| Flow | Amount | Unit |
|--|---------|------|
| metal working, average for steel product manufacturing - GLO | 1.00000 | kg |
| steel, low-alloyed - GLO | 1.00000 | kg |
| transport, freight train - Europe without Switzerland | 0.20000 | t*km |
| transport, freight, lorry 16-32 metric ton, EURO5 - GLO | 0.10000 | t*km |
| welding, arc, steel - GLO | 0.03260 | m |

Table 16 – LCI of stack frame, input data

| Flow | Amount | Unit |
|--------------------|----------------|-----------|
| Stack frame | 1.00000 | kg |

Table 17 – LCI of stack frame, output data

Energy subsystem

The energy subsystem includes both the electrolyte and the corresponding electrolyte tanks. To shape and manufacture the tank, the global market cut-off for extrusion of plastic film has been chosen.

Electrolyte tank

The vanadium electrolyte is stored in plastic tanks, and it is essential that these tanks are constructed from materials capable of withstanding the highly acidic environment. A combination of glass fiber with a PVC inline is chosen as a particularly suitable material. To manufacture the tank, the reference process "glass fiber reinforced plastic production, hand lay-up" is selected. The necessary quantities of glass fiber and PVC are computed based on the tank's dimensions, assuming a cylindrical shape [22].

| Flow | Amount | Unit |
|--|---------|------|
| ⚙️ chemical, organic - GLO | 0.02450 | kg |
| ⚙️ extrusion, plastic film - GLO | 0.02190 | kg |
| ⚙️ glass fibre - GLO | 0.62000 | kg |
| ⚙️ polyester resin, unsaturated - GLO | 0.41000 | kg |
| ⚙️ polyvinylchloride, bulk polymerised - GLO | 0.02190 | kg |
| ⚙️ transport, freight train - Europe without Switzerland | 0.21000 | t*km |
| ⚙️ transport, freight, lorry 16-32 metric ton, EURO5 - GLO | 0.11000 | t*km |
| ⚙️ transport, freight, sea, transoceanic ship - GLO | 1.06000 | t*km |

Table 18 – LCI of electrolyte tank, input data

| Flow | Amount | Unit |
|---|----------------|-----------|
| ⚙️ Tank | 1.00000 | kg |
| ⚙️ waste mineral wool, for final disposal - GLO | 0.05140 | kg |
| 🌿 Hydrocarbons, aromatic | 6.25000E-5 | kg |

Table 19 – LCI of electrolyte tank, output data

Electrolyte

The composition of the electrolyte is taken from the technical data of the manufacturer Gfe GmbH [22]. This VRFB employs an advanced electrolyte chemistry characterized by a sulfate-chloride-based complex formulation. Extensive testing has demonstrated that this electrolyte composition exhibits greater stability in comparison to conventional sulfate-based chemistry. Additionally, the electrolyte maintains stability across a broad temperature spectrum, ranging from 5 to 50°C, with minimal evolution of chlorine gas and other gases during operation. The constituents of the electrolyte include vanadium trichloride, hydrochloric acid, vanadium sulfate, vanadium oxide sulfate, sulfuric acid and water.

Vanadium salts are assumed to be derived from commercially available vanadium pentoxide (V_2O_5), a widely utilized compound in VRFB electrolyte preparation. The extraction and production processes of vanadium pentoxide, as described in the Weber et al.'s article, are considered identical for this study. The assumption is that vanadium is extracted from titanomagnetite ore containing 1.7% vanadium pentoxide. Following ore processing, vanadium-bearing magnetite is generated, necessitating pre-reduction. The pre-reduced vanadium pentoxide-bearing magnetite is then processed to yield cast iron, inclusive of vanadium pentoxide. This cast iron is typically used in steel production. In the course of this manufacturing process, slag is produced, with a V_2O_5 content of 25%, from which pure vanadium pentoxide is extracted. The corresponding LCI detailing the production of vanadium pentoxide, along with intermediate products, are provided from table 20 to table 29. The complete production phase has been adapted to South Africa, considering the electrolyte is made in that country [6].

- Vanadium bearing magnetite (2.2% V_2O_5 content)

Given the essential role of a comprehensive Life Cycle Inventory for the production of vanadium pentoxide in the Life Cycle Assessment of VRFB, a thorough model is developed for the entire process chain, including vanadium extraction and pentoxide production. Typically, vanadium derives from titanomagnetite ore, with pig iron being the primary product. The vanadium, concentrated in the

ore's slag, is recovered for further use. The Evraz Highveld Steel & Vanadium deposit in South Africa is a significant reference point for this process, producing titanomagnetite ore with a 1.7% vanadium pentoxide content. The subsequent production of vanadium pentoxide-bearing slags involves multiple steps. The mining operation is approximated using the Ecoinvent dataset "ilmenite-magnetite mine operation", with adjustments made to account for a 1.7% vanadium pentoxide content in the ore [22].

| Flow | Amount | Unit |
|--|-------------|-------------------|
| ⚙️ blasting - GLO | 0.00015 | kg |
| ⚙️ conveyor belt - GLO | 5.56000E-8 | m |
| ⚙️ diesel, burned in diesel-electric generating set - GLO | 0.02380 | MJ |
| ⚙️ electricity, medium voltage - ZA | 0.01440 | kWh |
| ⚙️ heat, central or small-scale, natural gas - RoW | 0.01540 | MJ |
| ⚙️ industrial machine, heavy, unspecified - GLO | 1.22000E-5 | kg |
| ⚙️ mine infrastructure, open cast, ilmenite from hard-rock ore - GLO | 3.08000E-11 | Item(s) |
| ⚙️ petrol, unleaded - RoW | 0.06270 | kg |
| ⚙️ recultivation, ilmenite mine - GLO | 8.29000E-5 | m ² |
| 🌿 Iron, 72% in magnetite, 14% in crude ore | 1.08000 | kg |
| 🌿 Occupation, mineral extraction site | 0.00249 | m ² *a |
| 🌿 TiO ₂ , 54% in ilmenite, 18% in crude ore | 0.25000 | kg |
| 🌿 Transformation, from forest | 8.29000E-5 | m ² |
| 🌿 Transformation, from mineral extraction site | 8.29000E-5 | m ² |
| 🌿 Vanadium ore | 0.03400 | kg |
| 🌿 Water, well, in ground | 5.86000E-5 | m ³ |

Table 20 – LCI of Vanadium bearing magnetite, input data

| Flow | Amount | Unit |
|---|----------------|----------------|
| ⚙️ Vanadium bearing magnetite | 1.53000 | kg |
| ⚙️ ilmenite, 54% titanium dioxide - GLO | 0.46000 | kg |
| 🌿 Particulates, < 2.5 um | 1.77000E-5 | kg |
| 🌿 Particulates, > 10 um | 0.00024 | kg |
| 🌿 Particulates, > 2.5 um, and < 10um | 9.57000E-5 | kg |
| 🌿 Water | 0.00879 | kg |
| 🌿 Water | 4.98000E-5 | m ³ |

Table 21 – LCI of Vanadium bearing magnetite, output data

- Pre-reduced vanadium pentoxide bearing magnetite

The titanomagnetite ore undergoes an initial pre-reduction process using coal at a temperature of 1000 °C within directly heated rotary kilns. As a benchmark process, the adapted Ecoinvent dataset titled "iron pellet production" is employed for reference [22].

| Flow | Amount | Unit |
|---|-------------|---------|
| ⚙️ Vanadium bearing magnetite | 1.53000 | kg |
| ⚙️ aluminium oxide factory - GLO | 2.50000E-11 | Item(s) |
| ⚙️ chromium - GLO | 5.97000E-6 | kg |
| ⚙️ dolomite - GLO | 0.00137 | kg |
| ⚙️ electricity, high voltage - ZA | 0.00229 | kWh |
| ⚙️ electricity, medium voltage - ZA | 0.02500 | kWh |
| ⚙️ hard coal ash - GLO | 0.01300 | kg |
| ⚙️ heat, district or industrial, natural gas - RoW | 0.06550 | MJ |
| ⚙️ heat, district or industrial, other than natural gas - RoW | 0.02330 | MJ |
| ⚙️ lime - GLO | 0.00057 | kg |
| ⚙️ lubricating oil - GLO | 4.60000E-7 | kg |
| ⚙️ sodium hydroxide, without water, in 50% solution state - GLO | 3.29000E-6 | kg |
| ⚙️ solvent, organic - GLO | 4.00000E-9 | kg |
| ⚙️ steel, unalloyed - GLO | 3.38000E-5 | kg |
| ⚙️ tap water - RoW | 0.02160 | kg |
| 🌊 Water | 9.00000E-5 | m3 |

Table 22 – LCI of pre-reduced V₂O₅ bearing magnetite, input data

| Flow | Amount | Unit |
|--|----------------|-----------|
| ⚙️ Pre-reduced V2O5 bearing magnetite | 1.46000 | kg |
| ⚙️ scrap steel - GLO | 3.26000E-6 | kg |
| ⚙️ spent solvent mixture - GLO | 1.23000E-7 | kg |
| ⚙️ waste mineral oil - GLO | 8.66000E-8 | kg |
| 🌊 Arsenic, ion | 6.20000E-12 | kg |
| 🌊 Cadmium | 2.10000E-10 | kg |
| 🌊 Cadmium, ion | 3.10000E-12 | kg |
| 🌊 Carbon dioxide, fossil | 0.02450 | kg |
| 🌊 Carbon monoxide, fossil | 0.00021 | kg |
| 🌊 Chromium | 2.70000E-9 | kg |
| 🌊 Chromium, ion | 4.96000E-11 | kg |
| 🌊 Cobalt | 6.20000E-12 | kg |
| 🌊 Copper | 4.60000E-9 | kg |
| 🌊 Copper, ion | 6.20000E-12 | kg |
| 🌊 Dinitrogen monoxide | 1.50000E-9 | kg |
| 🌊 Dioxins, measured as 2,3,7,8-tetrachlorodibenzo-p-dioxin | 5.70000E-15 | kg |
| 🌊 Hydrocarbons, aliphatic, alkanes, unspecified | 2.25000E-5 | kg |
| 🌊 Hydrogen chloride | 2.52000E-5 | kg |
| 🌊 Hydrogen fluoride | 2.04000E-5 | kg |
| 🌊 Iron, ion | 1.18000E-8 | kg |
| 🌊 Lead | 6.65000E-8 | kg |
| 🌊 Lead | 6.20000E-12 | kg |
| 🌊 Manganese | 2.30000E-8 | kg |
| 🌊 Manganese | 1.86000E-9 | kg |
| 🌊 Mercury | 3.49000E-10 | kg |
| 🌊 Mercury | 8.06000E-13 | kg |
| 🌊 Methane, fossil | 6.10000E-11 | kg |
| 🌊 Nickel | 1.50000E-8 | kg |

| | | |
|--|-------------|----|
| Nickel, ion | 6.20000E-12 | kg |
| Nitrate | 1.14000E-8 | kg |
| Nitrogen oxides | 0.00032 | kg |
| NMVOOC, non-methane volatile organic compounds, unspecified origin | 4.20000E-11 | kg |
| PAH, polycyclic aromatic hydrocarbons | 1.90000E-10 | kg |
| Particulates, < 2.5 um | 7.53000E-5 | kg |
| Particulates, > 10 um | 5.86000E-7 | kg |
| Particulates, > 2.5 um, and < 10um | 4.01000E-7 | kg |
| Phosphorus | 7.44000E-10 | kg |
| Silver | 5.64000E-11 | kg |
| Sulfur dioxide | 0.00013 | kg |
| Suspended solids, unspecified | 3.97000E-8 | kg |
| Water | 0.00325 | kg |
| Water | 1.84000E-5 | m3 |
| Zinc | 5.62000E-8 | kg |
| Zinc, ion | 2.48000E-11 | kg |

Table 23 – LCI of pre-reduced V₂O₅ bearing magnetite, output data

- V₂O₅ bearing cast iron

Subsequently, an additional reduction process is carried out in an electric arc furnace to acquire cast iron (pig iron), which retains the vanadium content from the ore (1.4% vanadium pentoxide in the iron). The energy requirements and auxiliary materials are sourced from a reference process in Ecoinvent, specifically "cast iron production" [22].

| Flow | Amount | Unit |
|---|-------------|---------|
| anode, for metal electrolysis - GLO | 0.00300 | kg |
| electric arc furnace converter - GLO | 4.00000E-11 | Item(s) |
| electricity, medium voltage - ZA | 0.42000 | kWh |
| hard coal ash - GLO | 0.01400 | kg |
| natural gas, high pressure - RoW | 0.02500 | m3 |
| oxygen, liquid - RoW | 0.05070 | kg |
| Pre-reduced V ₂ O ₅ bearing magnetite | 1.46000 | kg |
| quicklime, in pieces, loose - GLO | 0.05500 | kg |
| refractory, basic, packed - GLO | 0.01350 | kg |
| Water, unspecified natural origin, RoW | 0.00522 | m3 |

Table 24 – LCI of V₂O₅ bearing cast iron, input data

| Flow | Amount | Unit |
|--|----------------|-----------|
| ⚙️ V2O5 bearing cast iron | 1.32000 | kg |
| ⚙️ dust, alloyed electric arc furnace steel - GLO | 0.00960 | kg |
| ⚙️ inert waste, for final disposal - GLO | 0.00500 | kg |
| ⚙️ slag, unalloyed electric arc furnace steel - GLO | 0.09280 | kg |
| 🍃 Benzene | 2.31000E-6 | kg |
| 🍃 Cadmium | 3.65000E-8 | kg |
| 🍃 Carbon monoxide, fossil | 0.00232 | kg |
| 🍃 Chromium | 1.25000E-6 | kg |
| 🍃 Copper | 2.31000E-7 | kg |
| 🍃 Dioxins, measured as 2,3,7,8-tetrachlorodibenzo-p-dioxin | 4.54000E-12 | kg |
| 🍃 Hydrocarbons, aromatic | 7.70000E-5 | kg |
| 🍃 Hydrogen chloride | 5.20000E-6 | kg |
| 🍃 Hydrogen fluoride | 2.35000E-6 | kg |
| 🍃 Lead | 1.81000E-6 | kg |
| 🍃 Mercury | 2.24000E-6 | kg |
| 🍃 Nickel | 7.01000E-7 | kg |
| 🍃 Nitrogen oxides | 0.00018 | kg |
| 🍃 PAH, polycyclic aromatic hydrocarbons | 3.73000E-8 | kg |
| 🍃 Particulates, < 2.5 um | 0.00017 | kg |
| 🍃 Particulates, > 10 um | 5.86000E-5 | kg |
| 🍃 Particulates, > 2.5 um, and < 10um | 0.00017 | kg |
| 🍃 Polychlorinated biphenyls | 2.33000E-8 | kg |
| 🍃 Sulfur dioxide | 7.70000E-5 | kg |
| 🍃 Water | 2.02000 | kg |
| 🍃 Water | 0.00320 | m3 |
| 🍃 Zinc | 2.29000E-5 | kg |

Table 25 – LCI of V₂O₅ bearing cast iron, output data

- Vanadium slag (25% V₂O₅)

At the same time as the reduction process, a slag is generated, containing approximately 30% titanium dioxide, and it is deposited in slag piles. In a heat-resistant ladle, the molten pig iron undergoes oxidation using oxygen lances, causing the vanadium to transfer to the slag. The resulting slag comprises 25% vanadium pentoxide, serving as the primary raw material for vanadium production. To model this procedure, adjustments are made to the Ecoinvent dataset "steel production, electric arc furnace". The outputs of the process include steel and vanadium pentoxide-bearing slag. The quantity of the slag is tuned to achieve the targeted concentration of 25% vanadium pentoxide in the ladle slag. Furthermore, the allocation between the two by-products, vanadium slag and steel, is determined based on their respective market prices. Due to the absence of a market price for vanadium-bearing slag, an approximation is made using the market price for vanadium pentoxide and the corresponding V₂O₅ content in the slag [22].

| Flow | Amount | Unit |
|--|-------------|---------|
| ⚙ aluminium, wrought alloy - GLO | 1.48000E-5 | kg |
| ⚙ anode, for metal electrolysis - GLO | 0.00300 | kg |
| ⚙ argon, liquid - GLO | 0.00329 | kg |
| ⚙ cast iron - GLO | 5.15000E-5 | kg |
| ⚙ diesel, burned in building machine - GLO | 0.00346 | MJ |
| ⚙ electric arc furnace converter - GLO | 4.00000E-11 | Item(s) |
| ⚙ electricity, low voltage - ZA | 0.03460 | kWh |
| ⚙ electricity, medium voltage - ZA | 0.54000 | kWh |
| ⚙ ethylene glycol - GLO | 3.32000E-8 | kg |
| ⚙ ferrochromium, high-carbon, 68% Cr - GLO | 0.00011 | kg |
| ⚙ ferromanganese, high-coal, 74.5% Mn - GLO | 4.45000E-5 | kg |
| ⚙ ferrosilicon - GLO | 0.00370 | kg |
| ⚙ hard coal ash - GLO | 0.01400 | kg |
| ⚙ heat, district or industrial, natural gas - RoW | 1.23000 | MJ |
| ⚙ molybdenum trioxide - GLO | 1.41000E-5 | kg |
| ⚙ natural gas, high pressure - RoW | 0.02500 | m3 |
| ⚙ nickel, 99.5% - GLO | 3.32000E-5 | kg |
| ⚙ oxygen, liquid - RoW | 0.05070 | kg |
| ⚙ propane, burned in building machine - GLO | 0.00273 | MJ |
| ⚙ quicklime, in pieces, loose - GLO | 0.05500 | kg |
| ⚙ refractory, basic, packed - GLO | 0.01350 | kg |
| ⚙ slag, unalloyed electric arc furnace steel - GLO | 0.09280 | kg |
| ⚙ V2O5 bearing cast iron | 1.32000 | kg |
| ✔ Water, unspecified natural origin | 0.00522 | m3 |

Table 26 – LCI of vanadium slag, input data

| Flow | Amount | Unit |
|--|----------------|-----------|
| Vanadium slag (25 % V2O5) | 0.06130 | kg |
| dust, unalloyed electric arc furnace steel - GLO | 0.00960 | kg |
| inert waste, for final disposal - GLO | 0.00500 | kg |
| iron scrap, unsorted - GLO | 5.15000E-5 | kg |
| slag, unalloyed electric arc furnace steel - GLO | 0.04980 | kg |
| spent solvent mixture - GLO | 3.32000E-8 | kg |
| steel, low-alloyed - GLO | 1.20000 | kg |
| Argon-40 | 0.00329 | kg |
| Benzene | 2.29000E-6 | kg |
| Benzene, hexachloro- | 2.00000E-8 | kg |
| Cadmium | 3.65000E-8 | kg |
| Carbon monoxide, fossil | 0.00232 | kg |
| Chloride | 1.82000E-6 | kg |
| Chromium | 1.25000E-6 | kg |
| Chromium VI | 1.92000E-9 | kg |
| Copper | 2.31000E-7 | kg |
| Dioxins, measured as 2,3,7,8-tetrachlorodibenzo-p-dioxin | 4.54000E-12 | kg |
| Hydrocarbons, aromatic | 7.70000E-5 | kg |
| Hydrogen chloride | 5.20000E-6 | kg |
| Hydrogen fluoride | 2.35000E-6 | kg |
| Lead | 1.81000E-6 | kg |
| Mercury | 2.24000E-6 | kg |
| Nickel | 7.01000E-7 | kg |
| Nitrogen oxides | 0.00018 | kg |
| PAH, polycyclic aromatic hydrocarbons | 3.73000E-8 | kg |
| Particulates, < 2.5 um | 0.00017 | kg |
| Particulates, > 10 um | 5.86000E-5 | kg |
| Particulates, > 2.5 um, and < 10um | 0.00017 | kg |
| Polychlorinated biphenyls | 2.33000E-8 | kg |
| Sulfur dioxide | 7.70000E-5 | kg |
| Water | 2.92000 | kg |
| Water | 0.00230 | m3 |
| Zinc | 2.29000E-5 | kg |

Table 27 – LCI of vanadium slag, output data

- Production of 1 kg vanadium pentoxide (V_2O_5)

The latter part of the process chain focuses on producing vanadium pentoxide from the vanadium slag. The foundational approach for preparing vanadium pentoxide is based on information gathered from literature. The initial step involves grinding the obtained vanadium slag and removing iron granulates. The electricity requirements for these steps are drawn from analogous processes (grinding and crushing for aluminum oxide and sieving for soda ash).

Subsequently, the material is combined with sodium salts (Na_2SO_4 and Na_2CO_3) and subjected to roasting in a rotary kiln at 850°C. Emissions, including sulfur dioxide and carbon dioxide, are computed using stoichiometric relationships. The electricity and heat needed for operating the rotary kiln are obtained from a reference process related to phosphorus production.

After cooling, the roasted product undergoes leaching with water, involving the addition of sulfuric acid and ammonium at an elevated temperature. The intermediate product, ammonium polyvanadate, precipitates with an assumed yield of 90%. Additionally, sodium sulfate is produced

as a by-product. The electricity demand for this step is referenced to the digester in titanium dioxide production. Stoichiometric calculations determine the required input of sulfuric acid and the output of sodium sulfate. The leaching process includes filtration, assuming a 95% solid content in the filtered material. Electricity and heat demands for this process are derived from reference processes related to filtering and drying in a soda ash production process.

During this phase, a leached slag is obtained as waste. This leached slag is considered inert, and no specific waste treatment is considered. However, potential environmental risks from the leaching of contaminants into the soil and groundwater must be acknowledged if the slag is piled on heaps. The extracted raw vanadium compounds are further converted into high-purity vanadium pentoxide through roasting, with the heat and electricity demands for the kiln obtained from a reference process associated with phosphorus production.

The entire process occurs in South Africa [22].

| Flow | Amount | Unit |
|---|---------|------|
| ⚙ ammonium sulfate, as N - GLO | 0.31000 | kg |
| ⚙ electricity, medium voltage - ZA | 0.20000 | MJ |
| ⚙ heat, district or industrial, natural gas - RoW | 0.93000 | MJ |
| ⚙ soda ash, dense - GLO | 0.37000 | kg |
| ⚙ sodium sulfate, anhydrite - RoW | 0.50000 | kg |
| ⚙ sulfuric acid - GLO | 0.46000 | kg |
| ⚙ transport, freight train - RoW | 0.46000 | t*km |
| ⚙ transport, freight, lorry, unspecified - GLO | 0.07710 | t*km |
| ⚙ Vanadium slag (25 % V ₂ O ₅) | 1.35000 | kg |
| ⚙ water, deionised, from tap water, at user - GLO | 3.16000 | kg |

Table 28 – LCI of vanadium pentoxide, input data

| Flow | Amount | Unit |
|--|----------------|-----------|
| ⚙ Vanadium pentoxide (V₂O₅) | 1.00000 | kg |
| ⚙ iron scrap, unsorted - GLO | 0.06500 | kg |
| ⚙ sodium sulfate, anhydrite - GLO | 1.00000 | kg |
| ⚙ spent solvent mixture - GLO | 0.06320 | kg |
| 🗑 Carbon dioxide, fossil | 0.16000 | kg |
| 🗑 Oxygen, in air | 0.05640 | kg |
| 🗑 Slags | 0.47000 | kg |
| 🗑 Sulfur dioxide | 0.23000 | kg |
| 🗑 Water | 0.08450 | kg |

Table 29 – LCI of vanadium pentoxide, output data

- production of 1 kg vanadium sulfate mixture

The V₂O₅ is then employed in the production of necessary vanadium compounds for the electrolyte. Specifically, vanadium sulfate compounds, in the form of a tri- and tetravalent mixed vanadium compound (V₂(SO₄)₃ and VOSO₄), are manufactured and introduced into the electrolyte. The production process is guided by a patent [55].

Initially, vanadium pentoxide is combined with sulfur and concentrated sulfuric acid. Sulfur serves as a reducing agent for vanadium. Subsequently, the materials are kneaded together for 10 minutes using a mixer, resulting in a paste. This paste is then subjected to calcination within a temperature range of 150 to 440°C. The outcome is a mixture of tri- ($V_2(SO_4)_3$) and tetravalent (VO_2SO_4) vanadium compounds, with a molar ratio of approximately 1:1 [6].

| Flow | Amount | Unit |
|--|---------|-------|
| ⚙️ electricity, medium voltage - ZA | 0.30146 | ⚡ kWh |
| ⚙️ heat, district or industrial, natural gas - RoW | 1.81059 | 🔥 MJ |
| ⚙️ sulfur - GLO | 0.08840 | 📦 kg |
| ⚙️ sulfuric acid - GLO | 0.85635 | 📦 kg |
| ⚙️ Vanadium pentoxide (V2O5) | 0.50829 | 📦 kg |

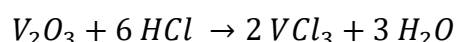
Table 30 – LCI of vanadium sulfate mixture, input data

| Flow | Amount | Unit |
|------------------------------------|----------------|-------------|
| ⚙️ Vanadium sulfate mixture | 1.00000 | 📦 kg |

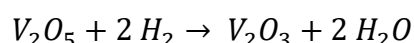
Table 31 – LCI of vanadium sulfate mixture, output data

- 1 kg vanadium trichloride

In this procedure, vanadium oxide is combined with hydrochloric acid, resulting in the production of vanadium trichloride and water, following the representation provided in Equation 1:



The preparation of vanadium trioxide is presumed to occur through the reduction of V_2O_5 in an hydrogen environment. The resultant reaction is expressed by Equation 2:



Finally, the last reaction is described by Equation 3:



Using the molar masses, the required inputs can be computed to produce vanadium trichloride. It is assumed that the electricity needed for the compound mixing process is negligible. However, since the Ecoinvent database only provides data for the liquid phase of hydrogen, electricity input must be taken into account to convert hydrogen from a liquid to a gaseous state. The production of hydrochloric acid (HCl) is chosen as a benchmark for the electricity input because, in this process, gaseous hydrogen is a primary energy requirement [6].

| Flow | Amount | Unit |
|--|---------|-------|
| ⚙️ electricity, medium voltage - ZA | 0.33000 | ⚡ kWh |
| ⚙️ hydrochloric acid, without water, in 30% solution state - RoW | 0.69536 | 📦 kg |
| ⚙️ hydrogen, liquid - RoW | 0.00641 | 📦 kg |
| ⚙️ Vanadium pentoxide (V2O5) | 0.57813 | 📦 kg |

Table 32 – LCI of vanadium trichloride, input data

| Flow | Amount | Unit |
|--------------------------------|----------------|-----------|
| ⚙️ Vanadium trichloride | 1.00000 | kg |
| 🌿 Water | 0.28632 | kg |

Table 33 – LCI of vanadium trichloride, output data

- 1 liter vanadium electrolyte

The Life Cycle Inventory (LCI) outcomes for the electrolyte can be found in Table 34-35.

| Flow | Amount | Unit |
|--|---------|------|
| ⚙️ hydrochloric acid, without water, in 30% solution state - RoW | 0.13500 | kg |
| ⚙️ sulfuric acid - GLO | 0.06750 | kg |
| ⚙️ transport, freight train - Europe without Switzerland | 0.12100 | t*km |
| ⚙️ transport, freight, inland waterways, barge - GLO | 0.17300 | t*km |
| ⚙️ transport, freight, lorry 16-32 metric ton, EURO5 - GLO | 0.02000 | t*km |
| ⚙️ transport, freight, lorry, unspecified - GLO | 0.18700 | t*km |
| ⚙️ transport, freight, sea, transoceanic ship - GLO | 3.81300 | t*km |
| ⚙️ Vanadium sulfate mixture | 0.13500 | kg |
| ⚙️ Vanadium trichloride | 0.13500 | kg |
| ⚙️ water, deionised, from tap water, at user - GLO | 0.87750 | kg |

Table 34 – LCI of vanadium electrolyte, input data

| Flow | Amount | Unit |
|-----------------------|----------------|-----------|
| ⚙️ Electrolyte | 1.35000 | kg |

Table 35 – LCI of vanadium electrolyte, output data

Periphery

The outer components include two copper cables, each measuring 5 meters, along with two pumps, a fan, pipes, a steel casing, an inverter, and a battery monitoring system (BMS). The copper cables have a cross-sectional area of 110 mm² and an insulation of 2 mm PVC. By considering the density of copper (8960 kg/m³) and PVC (1380 kg/m³), the overall cable mass and individual mass percentages can be computed. The attributes of the reference process, "cable production, unspecified", have been adapted to align with these specifications.

Copper cable

The copper cable needed for the cabling system consist of a copper component with PVC insulation. The computation of the material usage of copper and PVC is determined by the cable profile and the thickness of the insulation. The Life Cycle Inventory for cable production is derived from the Ecoinvent dataset labeled "cable production, unspecified". However, the input quantities of copper and PVC are tailored to their respective dimensions [22].

| Flow | Amount | Unit |
|--|-------------|-----------|
| ⚙️ copper - GLO | 0.94000 | 📦 kg |
| ⚙️ extrusion, plastic pipes - GLO | 0.06260 | 📦 kg |
| ⚙️ polyvinylchloride, bulk polymerised - GLO | 0.06260 | 📦 kg |
| ⚙️ rolling mill - GLO | 1.77000E-12 | 📦 Item(s) |
| ⚙️ tap water - Europe without Switzerland | 1.45000 | 📦 kg |
| ⚙️ transport, freight train - Europe without Switzerland | 0.19000 | 📦 t*km |
| ⚙️ transport, freight, lorry 16-32 metric ton, EURO5 - GLO | 0.09370 | 📦 t*km |
| ⚙️ wire drawing, copper - GLO | 0.94000 | 📦 kg |

Table 36 – LCI of copper cable, input data

| Flow | Amount | Unit |
|--|----------------|-------------|
| ⚙️ Copper cable | 1.00000 | 📦 kg |
| ⚙️ hazardous waste, for incineration - GLO | 0.00032 | 📦 kg |
| ⚙️ waste plastic, mixture - GLO | 0.00034 | 📦 kg |
| 🌿 Water | 0.00136 | 📦 m3 |
| 🌿 Water | 0.08860 | 📦 kg |

Table 37 – LCI of copper cable, output data

Pumps

To pump the electrolyte into the cells, two centrifugal pumps are necessary and redundantly arranged in each electrolyte circuit. The size and mass of the pump are determined using technical data sheets from commercial centrifugal pump providers, taking the flow rate as the foundation for subsequent calculations. The required material masses are adjusted accordingly, considering that the modeled VRFB pumps have an higher power [22].

| Flow | Amount | Unit |
|--|------------|-----------|
| ⚙️ aluminium, wrought alloy - GLO | 0.00825 | 📦 kg |
| ⚙️ cast iron - GLO | 0.49000 | 📦 kg |
| ⚙️ copper - GLO | 0.10000 | 📦 kg |
| ⚙️ hot water tank factory - GLO | 2.00000E-7 | 📦 Item(s) |
| ⚙️ polyvinylchloride, emulsion polymerised - GLO | 0.00158 | 📦 kg |
| ⚙️ polyvinylchloride, suspension polymerised - GLO | 0.01080 | 📦 kg |
| ⚙️ steel, chromium steel 18/8, hot rolled - GLO | 0.38000 | 📦 kg |
| ⚙️ synthetic rubber - GLO | 0.00289 | 📦 kg |
| ⚙️ transport, freight train - Europe without Switzerland | 0.20000 | 📦 t*km |
| ⚙️ transport, freight, lorry 16-32 metric ton, EURO5 - GLO | 0.10000 | 📦 t*km |

Table 38 – LCI of pumps, input data

| Flow | Amount | Unit |
|--|----------------|-------------|
| ⚙️ Pumps | 1.00000 | 📦 kg |
| ⚙️ waste plastic, mixture - GLO | 0.00289 | 📦 kg |
| ⚙️ waste polyvinylchloride product - GLO | 0.01240 | 📦 kg |

Table 39 – LCI of pumps, output data

Fan

The fan is manufactured by Digi-Key Electronics in Minnesota (USA) and details about its dimensions and materials are available in the fan's datasheet [56]. The fan has outer, inner, and blade diameters of 171.5 mm, 166 mm, and 162 mm, respectively. The frame and inner axis are made of aluminum, while the blades are constructed from glass fiber-reinforced polyamide-nylon. The fan features 4 wire leads, each measuring 365 mm. Assuming a cylindrical shape with a depth of 50.8 mm, the volumes of the aluminum frame and the inner axis can be calculated based on their inner and outer diameters.

Considering a schematic representation of the fan, it is reasonable to assume that the radius of the inner axis is half of the radius of the blades. This allows for the calculation of the volume of the inner axis. The blades, attached to the inner axis, are assumed to cover the surface of one circle with the given blade diameter, minus the diameter of the inner axis. The thickness of the blades is estimated to be approximately 4 mm.

The glass fiber-reinforced polyamide blades have a density of 1350 kg/m³, while aluminum has a density of about 2700 kg/m³. Using these densities, the mass fractions of both materials in the fan can be calculated. Given that the fan is produced in the USA, it is then transported to South Africa for the battery assembly [6].

| Flow | Amount | Unit |
|--|----------|------|
| aluminium, cast alloy - GLO | 0.34817 | kg |
| Copper cable | 0.61978 | kg |
| glass fibre reinforced plastic, polyamide, injection moulded - GLO | 0.03205 | kg |
| injection moulding - GLO | 0.34817 | kg |
| transport, freight, lorry 16-32 metric ton, EURO5 - GLO | 0.01821 | t*km |
| transport, freight, lorry, unspecified - GLO | 0.39002 | t*km |
| transport, freight, sea, transoceanic ship - GLO | 23.94250 | t*km |

Table 40 – LCI of fan, input data

| Flow | Amount | Unit |
|------------|----------------|-----------|
| Fan | 1.00000 | kg |

Table 41 – LCI of fan, output data

Pipes

The piping consists of steel pipes lined with Teflon. The necessary length of cables is determined based on the stack geometry, requiring 30 meters for each electrolyte circuit. Additionally, 5 meters of pipeline per stack are needed. It is assumed that a standard pipe with a diameter of 60.3 mm is used and the Teflon lining measures 1 mm. Using the density and dimensions, the required quantities of steel and Teflon can be calculated [22].

| Flow | Amount | Unit |
|---|---------|--------|
| ⚙ drawing of pipe, steel - GLO | 0.87000 | 📦 kg |
| ⚙ steel, chromium steel 18/8 - GLO | 0.87000 | 📦 kg |
| ⚙ tetrafluoroethylene film, on glass - GLO | 0.13000 | 📦 kg |
| ⚙ transport, freight train - Europe without Switzerland | 0.20000 | 📦 t*km |
| ⚙ transport, freight, lorry 16-32 metric ton, EURO5 - GLO | 0.10000 | 📦 t*km |

Table 42 – LCI of pipes, input data

| Flow | Amount | Unit |
|----------------|----------------|-------------|
| ⚙ Pipes | 1.00000 | 📦 kg |

Table 43 – LCI of pipes, output data

Battery monitoring system

The process control system for the VRFB comprises essential elements like cabling, panels, and a central unit. Given the absence of specific data on the exact composition of a process control system for a VRFB, the Life Cycle Inventory for a stationary lithium battery system is used as a reference. In the lithium battery system LCI, the process control system includes a stack monitoring interface and a battery monitoring system (BMS). The quantity of monitoring interfaces is contingent on the system's performance, while the BMS oversees up to 12 monitoring interfaces. In this context, the number of BMS components is adjusted to align with the performance of the VRFB system. It is assumed that one monitoring system is necessary per stack, thereby requiring one BMS to regulate them. It is crucial to acknowledge that this assumption represents a significant simplification, recognizing the process control system's importance. In reality, modeling the process control system is a critical aspect since electronics can potentially have substantial impacts in various categories. This substantial gap should be addressed in future research efforts [22].

- Stack monitoring interface

| Flow | Amount | Unit |
|---|---------|--------|
| ⚙ cable, data cable in infrastructure - GLO | 0.33000 | 📦 m |
| ⚙ cable, unspecified - GLO | 0.01930 | 📦 kg |
| ⚙ electronics, for control units - GLO | 0.15000 | 📦 kg |
| ⚙ injection moulding - GLO | 0.05000 | 📦 kg |
| ⚙ polypropylene, granulate - GLO | 0.05000 | 📦 kg |
| ⚙ sheet rolling, steel - GLO | 0.77000 | 📦 kg |
| ⚙ steel, low-alloyed - GLO | 0.77000 | 📦 kg |
| ⚙ transport, freight train - Europe without Switzerland | 0.60000 | 📦 t*km |
| ⚙ transport, freight, lorry 16-32 metric ton, EURO5 - GLO | 0.10000 | 📦 t*km |

Table 44 – LCI of stack monitoring interface, input data

| Flow | Amount | Unit |
|-------------------------------------|----------------|-------------|
| ⚙ Stack monitoring interface | 1.00000 | 📦 kg |

Table 45 – LCI of stack monitoring interface, output data

- Battery management system

| Flow | Amount | Unit |
|--|---------|--------|
| ⚙️ electronics, for control units - GLO | 0.32000 | 📦 kg |
| ⚙️ injection moulding - GLO | 0.18000 | 📦 kg |
| ⚙️ liquid crystal display, unmounted - GLO | 0.68000 | 📦 kg |
| ⚙️ polypropylene, granulate - GLO | 0.18000 | 📦 kg |
| ⚙️ transport, freight train - Europe without Switzerland | 0.60000 | 📦 t*km |
| ⚙️ transport, freight, lorry 16-32 metric ton, EURO5 - GLO | 0.10000 | 📦 t*km |

Table 46 – LCI of battery management system, input data

| Flow | Amount | Unit |
|-------------------------------------|----------------|-------------|
| ⚙️ Battery management system | 1.00000 | 📦 kg |

Table 47 – LCI of battery management system, output data

- Battery monitoring system

| Flow | Amount | Unit |
|-------------------------------|---------|------|
| ⚙️ Battery management system | 0.09000 | 📦 kg |
| ⚙️ Stack monitoring interface | 0.91000 | 📦 kg |

Table 48 – LCI of battery monitoring system, input data

| Flow | Amount | Unit |
|-------------------------------------|----------------|------------------|
| ⚙️ Battery monitoring system | 1.00000 | 📦 Item(s) |

Table 49 – LCI of battery monitoring system, output data

Steel housing

The steel housing is assumed to be entirely composed of steel, and the production process is approximated using the Ecoinvent dataset "sheet rolling, steel" [6].

| Flow | Amount | Unit |
|--|---------|--------|
| ⚙️ sheet rolling, steel - GLO | 1.00000 | 📦 kg |
| ⚙️ steel, low-alloyed - GLO | 1.00000 | 📦 kg |
| ⚙️ transport, freight train - Europe without Switzerland | 0.20000 | 📦 t*km |
| ⚙️ transport, freight, lorry 16-32 metric ton, EURO5 - GLO | 0.10000 | 📦 t*km |

Table 50 – LCI of steel housing, input data

| Flow | Amount | Unit |
|-------------------------|----------------|-------------|
| ⚙️ Steel housing | 1.00000 | 📦 kg |

Table 51 – LCI of steel housing, output data

5.2.2. Life cycle inventory for the manufacturing and transportation of VRFB

After the production of all VRFB components, it becomes essential to determine the quantity of each component required for the manufacturing of the entire battery system. The Life Cycle Inventory (LCI) detailing the manufacturing and transportation of the battery is presented in Table 52-53.

| Flow | Amount | Unit |
|--|------------|----------------|
| ⚙️ Bipolar plate | 159.55300 | kg |
| ⚙️ Cell frame | 8.89312 | kg |
| ⚙️ Copper cable | 11.05550 | kg |
| ⚙️ Current collector | 57.25310 | kg |
| ⚙️ Electrode | 12.17720 | kg |
| ⚙️ Electrolyte | 1524.00000 | kg |
| ⚙️ Fan | 2.60434 | kg |
| ⚙️ Gasket | 12.43880 | kg |
| ⚙️ Membrane | 4.35938 | kg |
| ⚙️ Pipes | 0.83452 | kg |
| ⚙️ Pumps | 5.00000 | kg |
| ⚙️ sawnwood, board, hardwood, air dried, planed - GLO | 0.12870 | m ³ |
| ⚙️ Stack frame | 36.41530 | kg |
| ⚙️ Steel housing | 337.72500 | kg |
| ⚙️ Tank | 43.20640 | kg |
| ⚙️ transport, freight, lorry 16-32 metric ton, EURO5 - GLO | 131.25200 | t*km |
| ⚙️ transport, freight, lorry 16-32 metric ton, EURO5 - GLO | 39.38000 | t*km |
| ⚙️ transport, freight, sea, transoceanic ship - GLO | 4.44372E4 | t*km |

Table 52 – LCI of manufacturing and transportation of VRFB, input data

| Flow | Amount | Unit |
|---|----------------|----------------|
| ⚙️ Manufactured & transported battery, VRB | 1.00000 | Item(s) |

Table 53 – LCI of manufacturing and transportation of VRFB, output data

Power subsystem

The mass of the components within the power subsystem is taken by Silva Lima et al.. In particular, Silva Lima et al.'s VRFB contains 40 cells, producing a nominal output power of 7.5 kW (although a maximum output of 14 kW is reported). Therefore, to generate 1 kW of power, about 5.33 cells are required. Using this ratio of 5.33, the mass of the power components for the VRFB under study can be calculated [6].

Energy subsystem

The electrolyte (with a total mass of 1524 kg) is divided into 662 kg for the catholyte and 862 kg for the anolyte. These quantities represent a volume of 1.13 m³, given the electrolyte's density of 1350 kg/m³. The tank holding the electrolyte has a height of 1.6 m, with the electrolyte filled with a height of 1.5 m, which corresponds to a total tank volume of 1.20 m³ and a void volume of 0.075 m³. Both anolyte and catholyte tanks are assumed to have identical dimensions, with each being a square, having a height, width, and depth of 1.6 m, 0.61 m and 0.61 m respectively [6].

Periphery

The cables consist of 9.86 kg of copper and 1.20 kg of PVC, so 11.06 kg per cable. Each pump weighs 2.5 kg and since both the catholyte and anolyte require one, a total of 5 kg for both pumps is needed in the battery system. The aluminum components of the fans, including the frame and inner axis, weigh 0.907 kg, while the blades add 0.083 kg, resulting in a total fan mass of 0.990 kg. Assuming the cables are not included in the fan's weight, which is 0.907 kg, the weight can be considered similar to the calculated mass. The 4 lead wires weigh 1.61 kg, for this reason the entire fan system weighs approximately 2.60 kg. Additionally, four pipes, each 1.5 m in length, are employed in the VRFB system. With a diameter of 25.4 mm and a thickness of 2 mm, the pipes have a combined mass of 0.83 kg.

All these components are enclosed within a steel housing, assuming it corresponds to the dimensions specified in the battery datasheet, measuring 0.75 m in width, 1.5 m in depth, and 2.0 m in height. With a wall thickness of 3 mm and a density of 7900 kg/m³, the steel housing weighs 337.73 kg. Particularly, the calculation began with the assumption that the total battery weight is 2.2 tonnes. The thickness of 3 mm was selected to match the information provided in the datasheet. Increasing the thickness by 1 mm would raise the total mass of the steel housing by approximately 100 kg [6].

Packaging and transport

The complete battery system is enclosed and shipped within a wooden crate weighing 90 kg. The packaging primarily uses hardwood, and for this purpose, the Ecoinvent process labeled "sawnwood, board, hardwood" has been selected, with a density of 699 kg/m³. It is assumed that the battery is manufactured entirely in South Africa and then directly transported to Italy [6].

5.2.3. Use phase

During the utilization phase, an inverter plays a crucial role in converting alternating current (AC) to direct current (DC) and vice versa. To fulfill the power requirements of the system, an inverter with an approximate capacity of 2.5 kW is chosen as a reference process. However, it is scaled up by a factor of 3 to match the power demand. Additionally, the battery control system is referred to as the "battery monitoring system".

The battery supplies 30 kWh of energy at a power output of 7.5 kW. It exhibits a round-trip efficiency of 83%, and a Depth of Discharge of 100%. With a lifespan of 20 years, the battery is expected to operate continuously throughout the designated time without a full replacement. However, occasional substitutions of some components may be required.

It is supposed that the battery undergoes 300 cycles per year. This estimation is based on the battery being charged and discharged once daily. However, it is considered that certain weather conditions may prevent the battery from being fully charged on certain days. Thus, 300 cycles per year are a more realistic value than the standard 365 cycles. Over a span of 20 years, the battery has provided a total of 180 MWh of energy, as demonstrated by the following equation:

$$30 \text{ kWh} \cdot 300 \text{ cycles} \cdot 20 \text{ years} = 180 \text{ MWh}$$

The electricity supplied must be processed from alternating current to direct current for the storage, and subsequently, it is converted back from DC to AC before being fed back into the grid. Throughout

this process, there are losses due to round-trip efficiency. The power converter operates at an efficiency rate of 96.5%, resulting in an overall efficiency of 77.29% when accounting for losses.

Furthermore, the battery requires electricity not only for charging but also for its various operational components such as pumps, fans and inverters. Considering charging and discharging times of 5 and 4 hours respectively, and assuming electricity is only required during battery operation, a total of 9 hours of electricity is needed for each cycle. Within these 9 hours, the battery consumes 500 W. Based on functional unit (1 MWh), 6000 cycles are assumed, resulting in an electricity demand of 27 MWh for the battery's operation.

According to the datasheets provided by some manufacturers, it is assumed that only the pumps and the fan require replacement during the 20 years operational period. The remaining components are expected to keep their quality during the entire lifetime. The pumps have a lifespan of 8 years, necessitating replacement after 8 and 16 years respectively. Each pump weighs 2.5 kg, resulting in a total mass of 5 kg for the replacement of two pumps, twice during the 20 year battery operation.

As for the fan, its datasheet indicates a lifespan of about 7 years. Thus, two new fans are required over the 20 years, with a mass of 5.21 kg. The fan's manufacturer is based in the USA, and it is assumed that the fan is transported by truck within the USA to the harbor, then shipped to Italy and finally transported by truck to the designated location.

Tables 54-55 provides the Life Cycle Inventory (LCI) for the use phase of the VRFB [6].

| Flow | Amount | Unit |
|---|-----------|---------|
| Battery monitoring system | 1.00000 | Item(s) |
| electricity, low voltage - IT | 52.88410 | MWh |
| electricity, low voltage - IT | 2.70000E4 | kWh |
| Fan | 5.21000 | kg |
| inverter, 2.5kW - GLO | 3.00000 | Item(s) |
| Manufactured & transported battery, VRB | 1.00000 | Item(s) |
| Pumps | 10.00000 | kg |
| transport, freight, lorry 16-32 metric ton, EURO5 - GLO | 4.97000 | t*km |
| transport, freight, lorry 16-32 metric ton, EURO5 - GLO | 0.31000 | t*km |
| transport, freight, lorry, unspecified - GLO | 2.03000 | t*km |
| transport, freight, sea, transoceanic ship - GLO | 41.95000 | t*km |

Table 54 – LCI of use phase of VRFB, input data

| Flow | Amount | Unit |
|---|------------------|------------|
| Electricity discharged (AC), photovoltaic energy support | 180.00000 | MWh |

Table 55 – LCI of use phase of VRFB, output data

5.2.4. End-of-life phase

Due to its early stage of development, the majority of VRFB components are constructed using entirely virgin materials. Unfortunately, there is limited understanding regarding the disassembly and recycling processes for these units [6].

Disposal of the stack

The stack comprises various components such as membranes, gaskets, cell frames, bipolar plates, electrodes, stack frame and current collectors, with a total mass of 291.1 kg. The Nafion membrane, a type of fluoropolymer, typically is processed in landfills or undergoes incineration, at the end of its life. Similarly, gaskets, made from materials containing fluorine, follow a similar disposal path. So, the disposal of the Nafion membrane and gaskets is specified using the Ecoinvent process "waste polyvinyl fluoride", representing disposal in a municipal solid waste incinerator.

In case of cell frame disposal, it is represented in OpenLCA by "market for waste polyvinyl chloride" process, involving treatment in both landfill and incineration in equal parts. Electrodes consist of plastic and carbon felt, while bipolar plates consist of plastic and synthetic graphite. For this reason, disposal of electrodes and bipolar plates is indicated by the "waste plastic, mixture" process, where 28% of plastic waste is incinerated, 24% landfilled and 48% employed for clinker production.

The stack frame, entirely steel-based, assumes only 5% disposal. Similarly, current collectors, entirely made of copper, follow the same assumption. Scrap steel is mostly landfilled, while scrap copper is predominantly incinerated. The following table shows the Life Cycle Inventory associated with stack disposal [6].










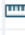



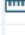

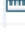
| Flow | Amount | Unit |
|--|----------------|--|
|  Stack treated | 1.00000 |  Item(s) |
|  diesel, burned in building machine - GLO | 29.10900 |  MJ |
|  electricity, medium voltage - IT | 2.91090 |  kWh |
|  scrap copper - GLO | 2.86266 |  kg |
|  scrap steel - GLO | 1.82077 |  kg |
|  waste plastic, mixture - GLO | 171.73000 |  kg |
|  waste polyvinylchloride - GLO | 8.89000 |  kg |
|  waste polyvinylfluoride - GLO | 16.80000 |  kg |

Table 56 – LCI of disposal of the stack

Disposal of the electrolyte

At present, electrolyte production is made by primary raw materials but in the future, electrolyte is expected to be recycled. For this purpose, only minor losses (assumed at 5%) during treatment are considered, approximated by the reference process "treatment of spent solvent mixture". In this case, the electrolyte is incinerated due to its classification as hazardous waste. The table illustrates the corresponding LCI [6].





| Flow | Amount | Unit |
|---|----------------|--|
|  Electrolyte treated | 1.00000 |  Item(s) |
|  spent solvent mixture - RoW | 76.20000 |  kg |

Table 57 – LCI of disposal of the electrolyte

Disposal of the periphery

The peripheral components are cables, pumps, fans, pipes, and the steel housing with a total weight of 365 kg. In particular, this amount includes two additional pumps and one fan, required as replacements over the 20 year period taken into account. Consequently, four pumps and two fans are assumed to become waste. However, the last two pumps and the last ordered fan are presumed to remain functional at the end of the 20 years and are thus excluded from waste treatment considerations.

End-of-life of cables consist of both copper cables from the system and those from the fans. The treatment process for used copper cable in the Ecoinvent database has been adapted to account for the mass of wire plastic insulation.

Disposal of pumps is divided into the two processes "waste polyvinylfluoride" and "waste polyvinylchloride". Fan disposal is composed by "waste aluminium", which is landfilled, and "waste plastic, mixture" representing the glass fiber reinforced plastic blades.

Pipes are considered non-reusable due to being made of plastic and thus the corresponding Ecoinvent dataset for "waste polypropylene" is employed, with larger part undergoes to landfill and only a small portion (10%) is incinerated. Additionally, 5% of the steel housing is landfilled. The comprehensive inventory for peripheral disposal is shown below [6].












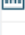

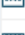

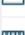



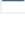
| Flow | Amount | Unit |
|--|----------------|--|
|  Periphery treated | 1.00000 |  Item(s) |
|  copper - GLO | 12.66970 |  kg |
|  diesel, burned in building machine - GLO | 36.48240 |  MJ |
|  electricity, medium voltage - IT | 3.64824 |  kWh |
|  scrap steel - GLO | 16.89000 |  kg |
|  waste aluminium - GLO | 1.81300 |  kg |
|  waste plastic, mixture - GLO | 0.08348 |  kg |
|  waste polypropylene - GLO | 0.83452 |  kg |
|  waste polyvinylchloride - GLO | 3.39000 |  kg |
|  waste polyvinylfluoride - GLO | 6.61000 |  kg |

Table 58 – LCI of disposal of the periphery

5.2.5. Final LCI for Vanadium Redox Flow Battery

The wooden packaging used for transporting the VRFB is introduced post-battery manufacturing, while the battery monitoring system and inverter are integrated in the use phase. Despite this, these elements are added into the end-of-life considerations for the VRFB. 40.878 MWh is the amount that represents the energy losses, since the overall efficiency of the battery is taken equal to 77.29%.

The comprehensive life cycle inventory for the VRFB, including these components and their disposal processes, is detailed in the following tables [6].

| Flow | Amount | Unit |
|---|----------|------|
| ⚙️ Electricity discharged (AC), photovoltaic energy support | 40.87800 | MWh |

Table 59 – Final LCI for VRFB, input data

| Flow | Amount | Unit |
|--|------------------|------------|
| ⚙️ Final VRFB LC | 180.00000 | MWh |
| ⚙️ used laptop computer - GLO | 0.01750 | kg |
| ⚙️ waste electric and electronic equipment - GLO | 0.10278 | kg |
| ⚙️ waste wood, untreated - RoW | 0.37500 | kg |
| 🗑️ Electrolyte treated | 0.00560 | Item(s) |
| 🗑️ Periphery treated | 0.00560 | Item(s) |
| 🗑️ Stack treated | 0.00560 | Item(s) |

Table 60 – Final LCI for VRFB, output data

5.3. Life cycle impact assessment (LCIA)

The assessment of the environmental impacts is made using ReCiPe 2016 Midpoint (H) calculation method, since it is one of the most employed in the past articles on LCA of VRFB. By considering the suggestions of Joint Research Center for a good LCIA of the products [57], 7 specific impact categories were taken into account for this LCA. The following graphs and tables show the main source of impact and percentual contributions for each compound of VRFB, respectively.

- *Impacts on Global warming*

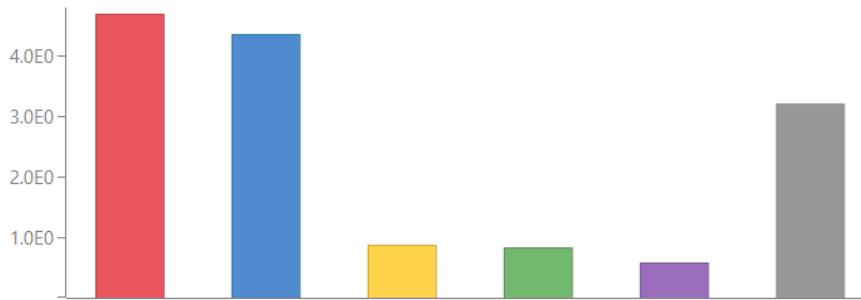


Figure 10 – Main contributors for global warming (in kg CO_{2eq}): (Red=electricity production, photovoltaic; Blue=tetrafluoroethylene; Yellow=inverter; Green=low-alloyed steel; Violet=hydrochloric acid; Grey=other)

| Contribution | Process | Total result [kg CO ₂ eq] |
|--------------|--|--------------------------------------|
| ✓ 100.06% | VRB Life Cycle | 14.52274 |
| ✓ 61.14% | Manufactured & transported battery, VRB | 8.87430 |
| > 19.44% | Membrane (Nafion) | 2.82210 |
| > 13.84% | Gasket FKM based | 2.00832 |
| > 08.44% | Electrolyte | 1.22441 |
| > 06.50% | Steel housing | 0.94372 |
| > 04.61% | Bipolar plate | 0.66846 |
| > 02.36% | Current collector | 0.34210 |
| > 01.69% | Electrolyte tank | 0.24525 |
| > 01.27% | Stack frame | 0.18382 |
| > 01.19% | Electrode | 0.17318 |
| > 00.45% | Copper cable | 0.06601 |
| > 00.38% | Pipes | 0.05552 |
| 00.26% | market for transport, freight, lorry 16-32 metric ton, EURO5, cut-off, S - GLO | 0.03702 |
| > 00.24% | Cell frame | 0.03547 |
| 00.20% | market for sawnwood, board, hardwood, air dried, planed, cut-off, S - GLO | 0.02860 |
| > 00.15% | Pumps | 0.02241 |
| > 00.12% | Fan | 0.01791 |
| 32.34% | electricity production, photovoltaic, 570kWp open ground installation, multi-Si, cut-off, S - IT | 4.69393 |
| 05.92% | market for inverter, 2.5kW, cut-off, S - GLO | 0.85912 |
| > 00.31% | Pumps | 0.04481 |
| > 00.25% | Fan | 0.03583 |
| > 00.09% | Battery monitoring system | 0.01325 |
| 00.01% | market for transport, freight, lorry 16-32 metric ton, EURO5, cut-off, S - GLO | 0.00115 |
| 00.00% | market for transport, freight, lorry, unspecified, cut-off, S - GLO | 0.00035 |
| > -00.00% | Periphery treatment | -0.00035 |
| > -00.02% | Stack treatment | -0.00302 |
| > -00.03% | Electrolyte treatment | -0.00485 |

Table 61 – Percentual contribution of global warming for each component of VRFB

As shown in the table, it's possible to note that about 60% of contribution in global warming is due to the manufacturing phase of VRFB, with Nafion membrane responsible for around 20%, due to the

presence of tetrafluoroethylene. For the same reason gasket has an higher percentage (~14%). Finally, the electricity production is accounted for 1/3 of total global warming impact.

- *Impacts on fine particulate matter formation*

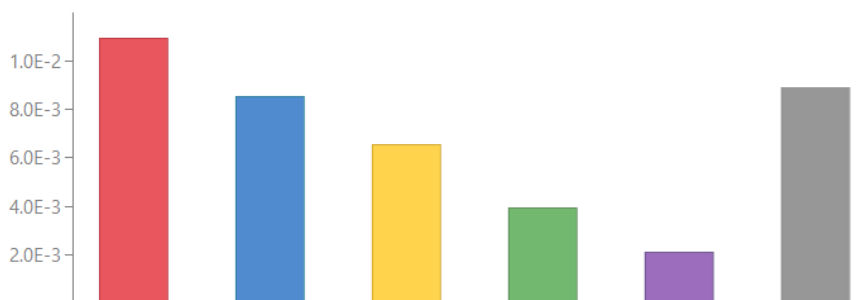


Figure 11 – Main contributors for fine particulate matter formation (in kg PM_{2.5eq}): (Red=electricity production, photovoltaic; Blue=copper; Yellow=V₂O₅; Green=inverter; Violet=low-alloyed steel; Grey=other)

| Contribution | Process | Total result [kg PM _{2.5 eq}] |
|--------------|--|---|
| 100.00% | VRB Life Cycle | 0.04100 |
| 62.03% | Manufactured & transported battery, VRB | 0.02544 |
| 24.61% | Electrolyte | 0.01009 |
| 16.94% | Current collector | 0.00694 |
| 05.54% | Steel housing | 0.00227 |
| 03.81% | Bipolar plate | 0.00156 |
| 03.09% | Copper cable | 0.00127 |
| 02.92% | Membrane (Nafion) | 0.00120 |
| 01.49% | Gasket FKM based | 0.00061 |
| 01.00% | Stack frame | 0.00041 |
| 00.94% | Electrolyte tank | 0.00038 |
| 00.54% | Electrode | 0.00022 |
| 00.50% | Fan | 0.00021 |
| 00.29% | Pumps | 0.00012 |
| 00.14% | market for sawnwood, board, hardwood, air dried, planed, cut-off, S - GLO | 5.57135E-5 |
| 00.11% | market for transport, freight, lorry 16-32 metric ton, EURO5, cut-off, S - GLO | 4.59403E-5 |
| 00.08% | Cell frame | 3.30205E-5 |
| 00.05% | Pipes | 2.14318E-5 |
| 26.68% | electricity production, photovoltaic, 570kWp open ground installation, multi-Si, cut-off, S - IT | 0.01094 |
| 09.62% | market for inverter, 2.5kW, cut-off, S - GLO | 0.00394 |
| 01.01% | Fan | 0.00041 |
| 00.58% | Pumps | 0.00024 |
| 00.08% | Battery monitoring system | 3.41978E-5 |
| 00.00% | market for transport, freight, lorry 16-32 metric ton, EURO5, cut-off, S - GLO | 1.42157E-6 |
| 00.00% | market for transport, freight, lorry, unspecified, cut-off, S - GLO | 5.90930E-7 |
| > 00.00% | Periphery treatment | 2.81754E-7 |
| > -00.00% | Stack treatment | -1.22482E-7 |
| > -00.00% | Electrolyte treatment | -1.29580E-6 |

Table 62 – Percentual contribution of fine particulate matter formation for each component of VRFB

Also in this case, manufactured battery represents ~60% of the impact, with a clear contribution of electrolyte and current collector, whose huge percentages are connected to vanadium pentoxide and copper, respectively. Around 27% of impacts on fine particulate matter formation is due to electricity production.

- Impacts on terrestrial acidification

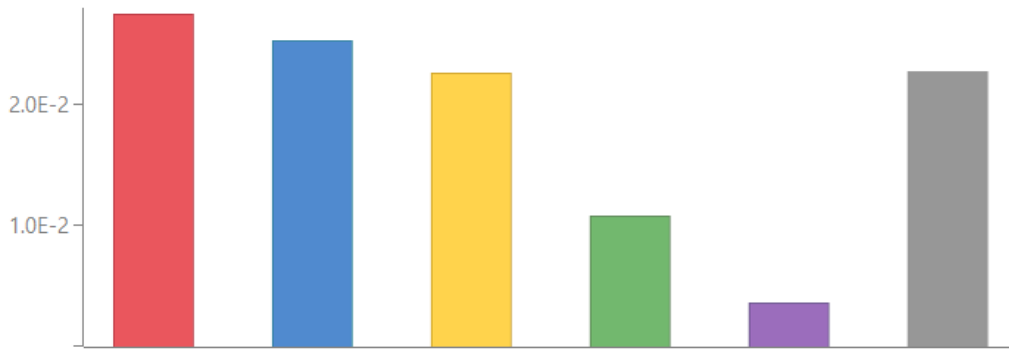


Figure 12 – Main contributors for terrestrial acidification (in kg SO_{2eq}): (Red=electricity production, photovoltaic; Blue=copper; Yellow=V₂O₅; Green=inverter; Violet= low-alloyed steel; Grey=other)

| Contribution | Process | Total result [kg SO ₂ eq] |
|--------------|--|--------------------------------------|
| ✓ 100.00% | VRB Life Cycle | 0.11232 |
| ✓ 64.37% | Manufactured & transported battery, VRB | 0.07230 |
| > 28.94% | Electrolyte | 0.03251 |
| > 18.32% | Current collector | 0.02058 |
| > 03.62% | Steel housing | 0.00406 |
| > 03.34% | Copper cable | 0.00375 |
| > 02.97% | Membrane (Nafion) | 0.00333 |
| > 02.50% | Bipolar plate | 0.00280 |
| > 01.51% | Gasket FKM based | 0.00169 |
| > 00.93% | Electrolyte tank | 0.00105 |
| > 00.74% | Stack frame | 0.00083 |
| > 00.54% | Fan | 0.00061 |
| > 00.41% | Electrode | 0.00046 |
| > 00.24% | Pumps | 0.00027 |
| 00.12% | market for sawnwood, board, hardwood, air dried, planed, cut-off, S - GLO | 0.00014 |
| 00.09% | market for transport, freight, lorry 16-32 metric ton, EURO5, cut-off, S - GLO | 9.88748E-5 |
| > 00.08% | Cell frame | 9.45050E-5 |
| > 00.03% | Pipes | 3.67287E-5 |
| 24.40% | electricity production, photovoltaic, 570kWp open ground installation, multi-Si, cut-off, S - IT | 0.02741 |
| 09.59% | market for inverter, 2.5kW, cut-off, S - GLO | 0.01077 |
| > 01.08% | Fan | 0.00121 |
| > 00.48% | Pumps | 0.00054 |
| > 00.08% | Battery monitoring system | 8.78462E-5 |
| 00.00% | market for transport, freight, lorry 16-32 metric ton, EURO5, cut-off, S - GLO | 3.05956E-6 |
| 00.00% | market for transport, freight, lorry, unspecified, cut-off, S - GLO | 1.39752E-6 |
| > 00.00% | Periphery treatment | 5.95032E-7 |
| > -00.00% | Stack treatment | -4.17255E-7 |
| > -00.00% | Electrolyte treatment | -3.42019E-6 |

Table 63 – Percentual contribution of terrestrial acidification for each component of VRFB

Impacts on terrestrial acidification presents very similar behavior, in terms of percentage, as fine particulate matter formation ones. Overall, 47% of the total of this category impact is connected to electrolyte and current collector, while electricity production is responsible for 24.4%.

- Impacts on mineral resource scarcity

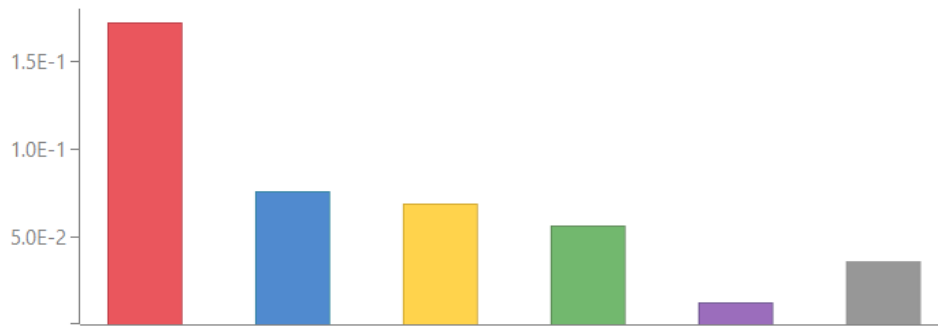


Figure 13 – Main contributors for mineral resource scarcity (in kg Cu_{eq}): (Red=copper; Blue=low-alloyed steel; Yellow=inverter; Green= electricity production, photovoltaic; Violet=chromium steel 18/8; Grey=other)

| Contribution | Process | Total result [kg Cu eq] |
|--------------|--|-------------------------|
| 100.00% | VRB Life Cycle | 0.41980 |
| 66.01% | Manufactured & transported battery, VRB | 0.27708 |
| 33.09% | Current collector | 0.13889 |
| 16.78% | Steel housing | 0.07043 |
| 06.00% | Copper cable | 0.02520 |
| 04.05% | Electrolyte | 0.01700 |
| 02.19% | Stack frame | 0.00920 |
| 01.24% | Pumps | 0.00520 |
| 00.88% | Fan | 0.00371 |
| 00.59% | Membrane (Nafion) | 0.00248 |
| 00.36% | Pipes | 0.00153 |
| 00.29% | Gasket FKM based | 0.00122 |
| 00.24% | Bipolar plate | 0.00100 |
| 00.17% | Electrolyte tank | 0.00070 |
| 00.07% | Electrode | 0.00030 |
| 00.03% | market for sawnwood, board, hardwood, air dried, planed, cut-off, S - GLO | 0.00013 |
| 00.02% | market for transport, freight, lorry 16-32 metric ton, EURO5, cut-off, S - GLO | 6.57296E-5 |
| 00.01% | Cell frame | 2.98655E-5 |
| 16.37% | market for inverter, 2.5kW, cut-off, S - GLO | 0.06871 |
| 13.25% | electricity production, photovoltaic, 570kWp open ground installation, multi-Si, cut-off, S - IT | 0.05561 |
| 02.48% | Pumps | 0.01039 |
| 01.77% | Fan | 0.00743 |
| 00.14% | Battery monitoring system | 0.00057 |
| 00.00% | market for transport, freight, lorry 16-32 metric ton, EURO5, cut-off, S - GLO | 2.03392E-6 |
| 00.00% | market for transport, freight, lorry, unspecified, cut-off, S - GLO | 6.71942E-7 |
| -00.00% | Periphery treatment | -8.49976E-8 |
| -00.00% | Stack treatment | -9.31442E-7 |
| -00.00% | Electrolyte treatment | -1.89386E-6 |

Table 64 – Percentual contribution of mineral resource scarcity for each component of VRFB

The current collector, due to the higher influence of copper, represents 1/3 of overall impacts on mineral resource scarcity, while inverter account for 16%, such as steel housing, whose low-alloyed steel has a great influence on it.

- Impacts on fossil resource scarcity

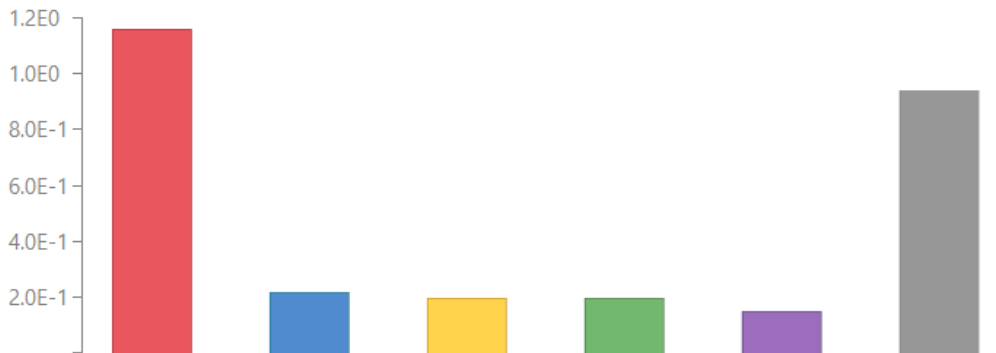


Figure 14 – Main contributors for fossil resource scarcity (in kg oil_{eq}): (Red=electricity production, photovoltaic; Blue=inverter; Yellow=low-alloyed steel; Green=graphite, battery grade; Violet=hydrochloric acid; Grey=other)

| Contribution | Process | Total result [kg oil eq] |
|--------------|--|--------------------------|
| ∨ 100.00% | VRB Life Cycle | 2.84327 |
| ∨ 50.98% | Manufactured & transported battery, VRB | 1.44937 |
| > 13.00% | Electrolyte | 0.36955 |
| > 10.68% | Bipolar plate | 0.30370 |
| > 08.02% | Steel housing | 0.22793 |
| > 04.63% | Membrane (Nafion) | 0.13168 |
| > 02.83% | Current collector | 0.08048 |
| > 02.79% | Electrode | 0.07937 |
| > 02.71% | Electrolyte tank | 0.07718 |
| > 02.53% | Gasket FKM based | 0.07205 |
| > 01.51% | Stack frame | 0.04301 |
| > 00.56% | Copper cable | 0.01605 |
| > 00.53% | Cell frame | 0.01518 |
| 00.45% | market for transport, freight, lorry 16-32 metric ton, EURO5, cut-off, S - GLO | 0.01270 |
| 00.31% | market for sawnwood, board, hardwood, air dried, planed, cut-off, S - GLO | 0.00887 |
| > 00.19% | Pumps | 0.00545 |
| > 00.16% | Fan | 0.00445 |
| > 00.06% | Pipes | 0.00173 |
| 40.64% | electricity production, photovoltaic, 570kWp open ground installation, multi-Si, cut-off, S - IT | 1.15545 |
| 07.55% | market for inverter, 2.5kW, cut-off, S - GLO | 0.21476 |
| > 00.38% | Pumps | 0.01090 |
| > 00.31% | Fan | 0.00891 |
| > 00.12% | Battery monitoring system | 0.00336 |
| 00.01% | market for transport, freight, lorry 16-32 metric ton, EURO5, cut-off, S - GLO | 0.00039 |
| 00.00% | market for transport, freight, lorry, unspecified, cut-off, S - GLO | 0.00012 |
| > 00.00% | Periphery treatment | 4.10672E-5 |
| > -00.00% | Stack treatment | -2.58867E-5 |
| > -00.01% | Electrolyte treatment | -0.00015 |

Table 65 – Percentual contribution of fossil resource scarcity for each component of VRFB

Regarding impacts on fossil fuel scarcity, ~50% is due to manufacturing phase, of which electrolyte represents 13%, bipolar plate around 11% (affected by the contribution of graphite) and steel housing 8% (because of low-alloyed steel that increase the percentage). Around 40% of the overall, is connected to electricity production, while inverter has a contribution equal to 7.5%.

- Impacts on human carcinogenic toxicity

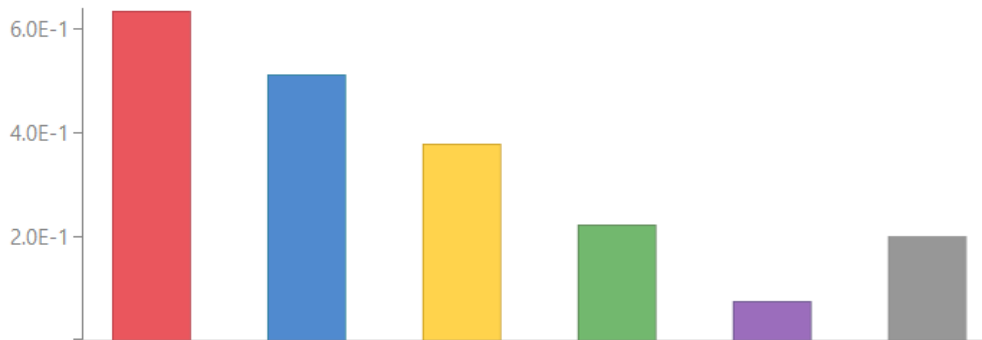


Figure 15 – Main contributors for human carcinogenic toxicity (in kg 1,4-DCB): (Red=low-alloyed steel; Blue=electricity production, photovoltaic; Yellow=copper; Green=inverter; Violet=sheet rolling, steel; Grey=other)

| Contribution | Process | Total result [kg 1,4-DCB] |
|--------------|--|---------------------------|
| ✓ 100.01% | VRB Life Cycle | 2.01343 |
| ✓ 61.25% | Manufactured & transported battery, VRB | 1.23318 |
| > 31.94% | Steel housing | 0.64301 |
| > 15.20% | Current collector | 0.30607 |
| > 03.94% | Stack frame | 0.07927 |
| > 02.76% | Copper cable | 0.05564 |
| > 02.34% | Electrolyte | 0.04721 |
| > 01.36% | Bipolar plate | 0.02746 |
| > 01.13% | Membrane (Nafion) | 0.02271 |
| > 00.69% | Pumps | 0.01389 |
| > 00.61% | Gasket FKM based | 0.01234 |
| > 00.44% | Fan | 0.00888 |
| > 00.38% | Electrolyte tank | 0.00775 |
| > 00.12% | Cell frame | 0.00234 |
| > 00.11% | Electrode | 0.00230 |
| > 00.11% | Pipes | 0.00226 |
| 00.07% | market for sawnwood, board, hardwood, air dried, planed, cut-off, S - GLO | 0.00132 |
| 00.04% | market for transport, freight, lorry 16-32 metric ton, EURO5, cut-off, S - GLO | 0.00073 |
| 25.41% | electricity production, photovoltaic, 570kWp open ground installation, multi-Si, cut-off, S - IT | 0.51165 |
| 10.92% | market for inverter, 2.5kW, cut-off, S - GLO | 0.21984 |
| > 01.38% | Pumps | 0.02778 |
| > 00.88% | Fan | 0.01776 |
| > 00.16% | Battery monitoring system | 0.00319 |
| 00.00% | market for transport, freight, lorry 16-32 metric ton, EURO5, cut-off, S - GLO | 2.27325E-5 |
| 00.00% | market for transport, freight, lorry, unspecified, cut-off, S - GLO | 7.73184E-6 |
| > -00.00% | Electrolyte treatment | -2.76902E-5 |
| > -00.00% | Periphery treatment | -5.42999E-5 |
| > -00.00% | Stack treatment | -7.06694E-5 |

Table 66 – Percentual contribution of human carcinogenic toxicity for each component of VRFB

Due to the higher influence in terms of carcinogenic effects, low-alloyed steel and copper largely influence the percentage of steel housing (~32%) and current collector (~15%), respectively. 25% of the contribution of human carcinogenic toxicity is represented by electricity production and 11% by inverter.

- Impacts on human non-carcinogenic toxicity

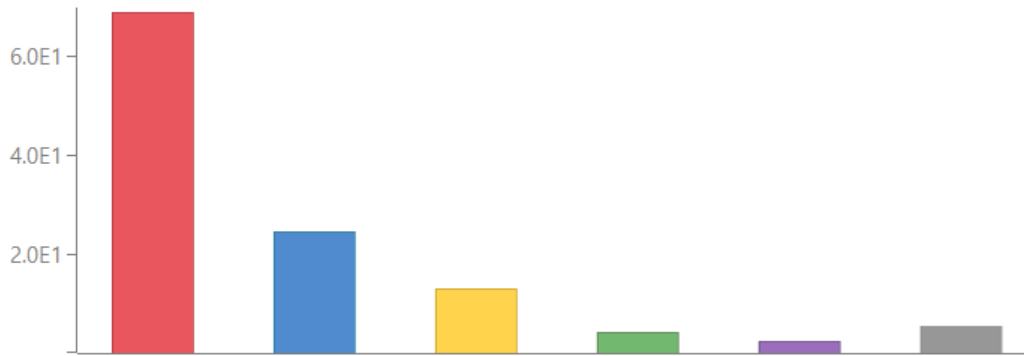


Figure 16 – Main contributors for human non-carcinogenic toxicity (in kg 1,4-DCB): (Red=copper; Blue=inverter; Yellow= electricity production, photovoltaic; Green=low alloyed steel; Violet=sheet rolling, copper; Grey=other)

| Contribution | Process | Total result [kg 1,4-DCB] |
|--------------|--|---------------------------|
| ∨ 100.02% | VRB Life Cycle | 118.03688 |
| ∨ 64.57% | Manufactured & transported battery, VRB | 76.20186 |
| > 47.14% | Current collector | 55.63005 |
| > 08.56% | Copper cable | 10.09865 |
| > 03.23% | Steel housing | 3.80734 |
| > 01.66% | Electrolyte | 1.95389 |
| > 01.26% | Fan | 1.48359 |
| > 00.68% | Membrane (Nafion) | 0.80309 |
| > 00.51% | Stack frame | 0.59915 |
| > 00.45% | Bipolar plate | 0.53454 |
| > 00.42% | Pumps | 0.49182 |
| > 00.35% | Gasket FKM based | 0.41375 |
| > 00.21% | Electrolyte tank | 0.24470 |
| > 00.05% | Electrode | 0.05669 |
| 00.03% | market for transport, freight, lorry 16-32 metric ton, EURO5, cut-off, S - GLO | 0.03223 |
| 00.03% | market for sawnwood, board, hardwood, air dried, planed, cut-off, S - GLO | 0.02978 |
| > 00.01% | Cell frame | 0.01153 |
| > 00.01% | Pipes | 0.01106 |
| 20.82% | market for inverter, 2.5kW, cut-off, S - GLO | 24.56509 |
| 11.07% | electricity production, photovoltaic, 570kWp open ground installation, multi-Si, cut-off, S - IT | 13.06616 |
| > 02.51% | Fan | 2.96794 |
| > 00.83% | Pumps | 0.98364 |
| > 00.21% | Battery monitoring system | 0.25089 |
| 00.00% | market for transport, freight, lorry 16-32 metric ton, EURO5, cut-off, S - GLO | 0.00100 |
| 00.00% | market for transport, freight, lorry, unspecified, cut-off, S - GLO | 0.00029 |
| > -00.00% | Electrolyte treatment | -0.00053 |
| > -00.00% | Periphery treatment | -0.00128 |
| > -00.02% | Stack treatment | -0.02149 |

Table 67 – Percentual contribution of human non-carcinogenic toxicity for each component of VRFB

In terms of non-carcinogenic toxicity, copper is the material that has the greatest impact in VRFB. In particular, current collector (made of copper) represents 47% of the overall impact, followed by inverter (~21%), electricity production (11%) and copper cable (8.5%).

6. DISCUSSION

In this chapter, considerations about the uncertainties and limitations on LCI of VRFB are discussed.

As mentioned in the chapter related to the state of art on LCA of VRFB, utilization phase plays a significant role to the overall impacts, but it needs additional research regarding life cycle inventory, because there are many discrepancies between the different articles. In particular in this analysis, the electricity discharged in alternate current is set equal to 180 MWh and it could be inaccurate since this parameter strongly depends on weather conditions.

Whenever possible, country-specific datasets in Ecoinvent have been selected. Alternatively, a dataset representing global market is chosen as the optimal substitute in instances where specificity is not achievable. In terms of electricity, since the battery is assumed to be used and disposed in Italy, the Italian electricity mix (medium and low voltage) is employed for these phases in the LCI, unlike the original inventory data of Silva Lima et al., which instead employed the energetic mix of Belgium (where use phase took place). The vanadium electrolyte processing, starting with titanomagnetite ore extraction in South Africa, made use of electricity mix of that country, for this reason in the LCI is selected the abbreviation “ZA” (meaning South Africa).

In LCI of Nafion membrane, the supplied heat input of 39.31 MJ/kg appears relatively high and could potentially lead to an overestimation of the impacts linked to membrane synthesis. Unfortunately, more precise information is not available. Due to the complexity of providing a detailed description of the entire process, a simplified method is adopted [22]. Impact analysis shows that the membrane contributes significantly to the total impact; in fact, Nafion is responsible of nearly 20% of the overall impact on global warming of VRFB, mainly because of the presence of tetrafluoroethylene. As stated by Weber et al.'s study, a hypothetical way to reduce this impact is to employ sulfonated polyether ether ketone (SPEEK) that stands out as a highly promising substitute for the conventional Nafion membrane material.

To simplify the stoichiometric calculation of pan-based electrode, it is presumed that the resultant carbon felt is predominantly composed of carbon. In the absence of LCI data regarding the composition of the emitted gases, only the carbon component is considered in the balance, with the assumption that the exhaust gas undergoes purification through a regenerative thermal oxidizer (RTO) [22].

In case of gaskets, the respective Ecoinvent datasets for the chemicals are used, with hexafluoropropylene replaced for simplicity by hexafluoroethane and vinylidene fluoride by polyvinylfluoride [22]. In addition, FKM (fluoroelastomer) is considered the standard material for the base-case configuration of gaskets and is taken into account in this LCI. However, according to Weber et al., different hypothetical materials for gaskets could be available in VRFB scenario, for example EPDM (ethylene propylene diene monomer) and silicone; these two materials are less commonly used, but could significantly reduce the impacts on global warming associated with the VRFB gaskets [22].

Detailed information on the extraction and processing of vanadium is not available in either literature or Ecoinvent, so using technical data of the manufacturer is the only way to conduct a proper LCI [22]. Throughout the production process of 1 kg vanadium sulfate, it is assumed that the

electricity and heat requirements align with those of producing 1 kg of soda ash, following the modified Solvay process [58]. This assumption is made because both processes involve a calcination step, which is identified as the most electricity-intensive process [6].

As there is no precise information on the specific composition of materials for centrifugal pump production, a reference process from Ecoinvent (pump production, 40 W) is used for guidance. Regarding LCI of pipes, there is no specific dataset for Teflon, so tetrafluoroethylene is used as an approximation [22].

One of the main gaps about LCI of VRFB is about battery monitoring system. Given the absence of specific data on the exact composition of a process control system for a VRFB, the life cycle inventory for a stationary lithium battery system is used as a reference [22].

The inverter, used to convert alternating current to direct current and vice versa, is essential for the primary connections of the battery system. Since there's no dependable data regarding the composition and manufacturing of an inverter specific to VRFB, the standard Ecoinvent dataset is utilized and adjusted to match the appropriate power rating [22].

Additionally, processes from the Ecoinvent database such as "treatment of waste wood, untreated", "used laptop computer" and "waste electric and electronic equipment" are employed for managing the wood packaging, battery monitoring system and inverter, respectively.

The emissions of substances shown in several outputs in LCI for the VRFB compounds are expressed in OpenLCA as elementary flows. The two big categories of elementary flows taken into account in the analysis are "emission to water" and "emission to air". Unfortunately, in the literature there are not specified information regarding the specific destination of these elementary flows, for example in the case of emission to water, there are several options in the software like emission to lake, ground water, river, ocean and so on. For this reason, the option "unspecified" was set for every elementary flow.

In life cycle assessment, it is a standard procedure to include the effects of recycling within the life cycle analysis. This involves substituting recycled materials for the extraction of raw materials and subsequent processing into the necessary materials. In this case, only treatment processes aimed at the safe disposal of non-recycled battery components are accounted for. Nowadays, there is limited understanding regarding the disassembly and recycling processes for the components of VRFB. In particular, vanadium is considered a critical raw material by the European Union. Critical raw materials are those that are of high economic importance to the EU, but with a high risk associated with their supply. These materials are crucial for the development of strategic sectors like clean energy, high-tech industries and digitalization. For this reason recycling of VRFB become a key factor for the future. According to the latest research, vanadium electrolyte is expected to be recycled for the next few years [6]. Finally, due to the massive presence of metals (such as copper and steel) and plastics, a suggestion for a more complete LCI in the coming years is to include their recycling and reuse.

In terms of transport, there are many uncertainties in literature that could be taken into account. Above all, the specific path of vanadium electrolyte from South Africa to Italy was not investigated, so at the moment many approximations were made. Whenever transportation via truck is utilized in

LCI, the process labeled "transport, freight, lorry 16-32 metric ton, EURO5" is employed, even if EURO6 emission standards are currently applied in the EU.

7. Conclusions

This paper contributes to knowledge and awareness on vanadium redox flow batteries, especially in terms of inventory data analysis.

Furthermore, the thesis lays the foundations for future developments and calculations of environmental impacts, in compliance with the objectives and guidelines of the European Commission (i.e. Product Environmental Footprint Category Rules and battery passport), as it identifies which variables present more uncertainty, which data are missing and which are more established in terms of quantity and also correspondence in the Ecoinvent database. These aspects are very important, as currently these types of batteries are usually only marginally studied, especially when compared to lithium-ion batteries.

The increasing number of reviews on technology and LCA of VRFB shows a tendency for the adoption of this redox flow battery rather than others and the need to compete with Li-ion batteries, which are currently considered by many to be the most promising batteries. The exponential growth in review papers published over the last few years is not only a consequence of this fact, but also because the VRFB configuration involves the synergy of multiple fields of science and technology. However it is necessary to further promote the research about the sustainability of this kind of technology in order to better understand its use on a world scale.

Nevertheless, VRFB already has one of the biggest power capacities installed on commercial facilities when compared to other energy storage technologies. All these achievements lead us to believe that in the short/medium term this type of battery will exhibit a substantial reduction in its price, which will contribute to making it an even more interesting and low-cost green technology for energy storage at different scales and in different sectors [59].

BIBLIOGRAPHY

- [1] J. Gouveia, A. Mendes, R. Monteiro, T. M. Mata, N. S. Caetano, and A. A. Martins, "Life cycle assessment of a vanadium flow battery," in *Energy Reports*, Elsevier Ltd, Feb. 2020, pp. 95–101. doi: 10.1016/j.egy.2019.08.025.
- [2] Ritchie H, Rosado P, and Roser M, "CO₂ and Greenhouse Gas Emissions."
- [3] Intergovernmental Panel on Climate Change, *Climate change 2014 : synthesis report : longer report*.
- [4] "EUROPEAN GREEN DEAL".
- [5] A. A. Kebede, T. Kalogiannis, J. Van Mierlo, and M. Bercibar, "A comprehensive review of stationary energy storage devices for large scale renewable energy sources grid integration," *Renewable and Sustainable Energy Reviews*, vol. 159. Elsevier Ltd, May 01, 2022. doi: 10.1016/j.rser.2022.112213.
- [6] L. da Silva Lima *et al.*, "Life cycle assessment of lithium-ion batteries and vanadium redox flow batteries-based renewable energy storage systems," *Sustainable Energy Technologies and Assessments*, vol. 46, Aug. 2021, doi: 10.1016/j.seta.2021.101286.
- [7] D. Baur, M. J. Baumann, P. Stuhm, and M. Weil, "Societal Acceptability of Large Stationary Battery Storage Systems," *Energy Technology*, vol. 11, no. 6, Jun. 2023, doi: 10.1002/ente.202201454.
- [8] O. Folorunso, P. O. Olukanmi, and T. Shongwe, "Progress towards sustainable energy storage: A concise review," *Engineering Reports*. John Wiley and Sons Inc, 2023. doi: 10.1002/eng2.12731.
- [9] E. Craddock, R. M. Cuéllar-Franca, and M. Pérez-Page, "The incorporation of 2D materials into membranes to improve the environmental sustainability of vanadium redox flow batteries (VRFBs): A critical review," *Current Opinion in Chemical Engineering*, vol. 40. Elsevier Ltd, Jun. 01, 2023. doi: 10.1016/j.coche.2023.100906.
- [10] T. Puleston, A. Clemente, R. Costa-Castelló, and M. Serra, "Modelling and Estimation of Vanadium Redox Flow Batteries: A Review," *Batteries*, vol. 8, no. 9. MDPI, Sep. 01, 2022. doi: 10.3390/batteries8090121.
- [11] A. Aluko and A. Knight, "A Review on Vanadium Redox Flow Battery Storage Systems for Large-Scale Power Systems Application", doi: 10.1109/ACCESS.2022.0092316.
- [12] I. Mayrhuber, C. R. Dennison, V. Kalra, and E. C. Kumbur, "Laser-perforated carbon paper electrodes for improved mass-transport in high power density vanadium redox flow batteries," *J Power Sources*, vol. 260, pp. 251–258, Aug. 2014, doi: 10.1016/J.JPOWSOUR.2014.03.007.
- [13] S. Kumar and S. Jayanti, "Effect of flow field on the performance of an all-vanadium redox flow battery," *J Power Sources*, vol. 307, pp. 782–787, Mar. 2016, doi: 10.1016/J.JPOWSOUR.2016.01.048.
- [14] K. Yaji, S. Yamasaki, S. Tsushima, T. Suzuki, and K. Fujita, "Topology optimization for the design of flow fields in a redox flow battery," *Structural and Multidisciplinary Optimization*, vol. 57, no. 2, pp. 535–546, Feb. 2018, doi: 10.1007/s00158-017-1763-8.
- [15] C. H. Chen, K. Yaji, S. Yamasaki, S. Tsushima, and K. Fujita, "Computational design of flow fields for vanadium redox flow batteries via topology optimization," *J Energy Storage*, vol. 26, p. 100990, Dec. 2019, doi: 10.1016/J.EST.2019.100990.

- [16] X. Ma, H. Zhang, C. Sun, Y. Zou, and T. Zhang, "An optimal strategy of electrolyte flow rate for vanadium redox flow battery," *J Power Sources*, vol. 203, pp. 153–158, Apr. 2012, doi: 10.1016/J.JPOWSOUR.2011.11.036.
- [17] C. Zhang, T. S. Zhao, Q. Xu, L. An, and G. Zhao, "Effects of operating temperature on the performance of vanadium redox flow batteries," *Appl Energy*, vol. 155, pp. 349–353, Oct. 2015, doi: 10.1016/J.APENERGY.2015.06.002.
- [18] Y. Kim *et al.*, "Activity gradient carbon felt electrodes for vanadium redox flow batteries," *J Power Sources*, vol. 408, pp. 128–135, Dec. 2018, doi: 10.1016/J.JPOWSOUR.2018.09.066.
- [19] H. R. Jiang, B. W. Zhang, J. Sun, X. Z. Fan, W. Shyy, and T. S. Zhao, "A gradient porous electrode with balanced transport properties and active surface areas for vanadium redox flow batteries," *J Power Sources*, vol. 440, p. 227159, Nov. 2019, doi: 10.1016/J.JPOWSOUR.2019.227159.
- [20] S. Tsushima and T. Suzuki, "Modeling and Simulation of Vanadium Redox Flow Battery with Interdigitated Flow Field for Optimizing Electrode Architecture," *J Electrochem Soc*, vol. 167, no. 2, p. 020553, Jan. 2020, doi: 10.1149/1945-7111/ab6dd0.
- [21] Q. He *et al.*, "Modeling of vanadium redox flow battery and electrode optimization with different flow fields," *e-Prime - Advances in Electrical Engineering, Electronics and Energy*, vol. 1, Jan. 2021, doi: 10.1016/j.prime.2021.100001.
- [22] S. Weber, J. F. Peters, M. Baumann, and M. Weil, "Life Cycle Assessment of a Vanadium Redox Flow Battery," *Environ Sci Technol*, vol. 52, no. 18, pp. 10864–10873, Sep. 2018, doi: 10.1021/acs.est.8b02073.
- [23] H. He, S. Tian, B. Tarroja, O. A. Ogunseitan, S. Samuelsen, and J. M. Schoenung, "Flow battery production: Materials selection and environmental impact," *J Clean Prod*, vol. 269, Oct. 2020, doi: 10.1016/j.jclepro.2020.121740.
- [24] S. Ebner, S. Spirk, T. Stern, and C. Mair-Bauernfeind, "How Green are Redox Flow Batteries?," *ChemSusChem*, vol. 16, no. 8. John Wiley and Sons Inc, Apr. 21, 2023. doi: 10.1002/cssc.202201818.
- [25] International Standard Organization, "ISO 14040:2006 Environmental management — Life cycle assessment — Principles and framework," 2006.
- [26] International Standard Organization, "ISO 14044:2006 Environmental management — Life cycle assessment — Requirements and guidelines," 2006.
- [27] Joint Research Center, "ILCD handbook," *European Commission*, 2010.
- [28] R. Yudhistira, D. Khatiwada, and F. Sanchez, "A comparative life cycle assessment of lithium-ion and lead-acid batteries for grid energy storage," *J Clean Prod*, vol. 358, Jul. 2022, doi: 10.1016/j.jclepro.2022.131999.
- [29] General Secretariat of the European Council, "Proposal for a Regulation of the European Parliament and of the Council concerning batteries and waste batteries, repealing Directive 2006/66/EC and amending Regulation (EU) No 2019/1020," 2023.
- [30] Stefan Kupferschmid and Usama Khalid, "EU Battery Regulation: Carbon Footprint Calculations in Focus," *Sphera*.
- [31] Andrea Casas Ocampo, "NEW EUROPEAN BATTERY REGULATION," *CIC energiGUNE*.

- [32] P. L'Abbate, M. Dassisti, and A. G. Olabi, "Small-Size Vanadium Redox Flow Batteries: An Environmental Sustainability Analysis via LCA," in *Green Energy and Technology*, Springer Verlag, 2019, pp. 61–78. doi: 10.1007/978-3-319-93740-3_5.
- [33] C. Mostert, B. Ostrander, S. Bringezu, and T. M. Kneiske, "Comparing electrical energy storage technologies regarding their material and carbon footprint," *Energies (Basel)*, vol. 11, no. 12, Dec. 2018, doi: 10.3390/en11123386.
- [34] J. R. Gouveia, E. Silva, T. M. Mata, A. Mendes, N. S. Caetano, and A. A. Martins, "Life cycle assessment of a renewable energy generation system with a vanadium redox flow battery in a NZEB household," *Energy Reports*, vol. 6, pp. 87–94, Feb. 2020, doi: 10.1016/j.egy.2019.08.024.
- [35] C. J. Rydh, "Environmental assessment of vanadium redox and lead-acid batteries for stationary energy storage."
- [36] M. AlShafi and Y. Bicer, "Life cycle assessment of compressed air, vanadium redox flow battery, and molten salt systems for renewable energy storage," *Energy Reports*, vol. 7, pp. 7090–7105, Nov. 2021, doi: 10.1016/j.egy.2021.09.161.
- [37] E. Shittu *et al.*, "Life cycle assessment of soluble lead redox flow battery," *J Clean Prod*, vol. 337, p. 130503, Feb. 2022, doi: 10.1016/J.JCLEPRO.2022.130503.
- [38] N. Blume, M. Becker, T. Turek, and C. Minke, "Life cycle assessment of an industrial-scale vanadium flow battery," *J Ind Ecol*, vol. 26, no. 5, pp. 1796–1808, Oct. 2022, doi: 10.1111/jiec.13328.
- [39] L. Unterreiner, V. Jülch, and S. Reith, "Recycling of Battery Technologies - Ecological Impact Analysis Using Life Cycle Assessment (LCA)," in *Energy Procedia*, Elsevier Ltd, 2016, pp. 229–234. doi: 10.1016/j.egypro.2016.10.113.
- [40] M. Hiremath, K. Derendorf, and T. Vogt, "Comparative Life Cycle Assessment of Battery Storage Systems for Stationary Applications," 2015.
- [41] L. Stougie *et al.*, "Multi-dimensional life cycle assessment of decentralised energy storage systems," *Energy*, vol. 182, pp. 535–543, Sep. 2019, doi: 10.1016/J.ENERGY.2019.05.110.
- [42] M. Baumann, J. Peters, and M. Weil, "Exploratory Multicriteria Decision Analysis of Utility-Scale Battery Storage Technologies for Multiple Grid Services Based on Life-Cycle Approaches," *Energy Technology*, vol. 8, no. 11, Nov. 2020, doi: 10.1002/ente.201901019.
- [43] U. Geological Survey, "MINERAL COMMODITY SUMMARIES 2022," 2022.
- [44] R. E. Ciez and J. F. Whitacre, "Examining different recycling processes for lithium-ion batteries," *Nat Sustain*, vol. 2, no. 2, pp. 148–156, Feb. 2019, doi: 10.1038/s41893-019-0222-5.
- [45] J. Quan, S. Zhao, D. Song, T. Wang, W. He, and G. Li, "Comparative life cycle assessment of LFP and NCM batteries including the secondary use and different recycling technologies," *Science of The Total Environment*, vol. 819, p. 153105, May 2022, doi: 10.1016/J.SCITOTENV.2022.153105.
- [46] M. Dassisti, G. Cozzolino, M. Chimienti, A. Rizzuti, P. Mastrorilli, and P. L'abbate, "Sustainability of vanadium redox-flow batteries: Benchmarking electrolyte synthesis procedures."
- [47] M. Baumann, J. F. Peters, M. Weil, and A. Grunwald, "CO2 Footprint and Life-Cycle Costs of Electrochemical Energy Storage for Stationary Grid Applications," *Energy Technology*, vol. 5, no. 7, pp. 1071–1083, Jul. 2017, doi: 10.1002/ente.201600622.

- [48] M. C. Díaz-Ramírez, V. J. Ferreira, T. García-Armingol, A. M. López-Sabirón, and G. Ferreira, "Battery manufacturing resource assessment to minimise component production environmental impacts," *Sustainability (Switzerland)*, vol. 12, no. 17, Sep. 2020, doi: 10.3390/SU12176840.
- [49] C. Jones, P. Gilbert, and L. Stamford, "Assessing the Climate Change Mitigation Potential of Stationary Energy Storage for Electricity Grid Services," *Environ Sci Technol*, 2019, doi: 10.1021/acs.est.9b06231.
- [50] M. C. Díaz-Ramírez, M. Blecua-de-Pedro, A. J. Arnal, and J. Post, "Acid/base flow battery environmental and economic performance based on its potential service to renewables support," *J Clean Prod*, vol. 330, Jan. 2022, doi: 10.1016/j.jclepro.2021.129529.
- [51] C. M. Fernandez-Marchante, M. Millán, J. I. Medina-Santos, and J. Lobato, "Environmental and Preliminary Cost Assessments of Redox Flow Batteries for Renewable Energy Storage," *Energy Technology*, vol. 8, no. 11, Nov. 2020, doi: 10.1002/ente.201900914.
- [52] A. Sternberg and A. Bardow, "Power-to-What? - Environmental assessment of energy storage systems," 2015.
- [53] M. C. Díaz-Ramírez, V. J. Ferreira, T. García-Armingol, A. M. López-Sabirón, and G. Ferreira, "Environmental assessment of electrochemical energy storage device manufacturing to identify drivers for attaining goals of sustainable materials 4.0," *Sustainability (Switzerland)*, vol. 12, no. 1, Jan. 2020, doi: 10.3390/su12010342.
- [54] M. A. Morales-Mora, J. J. H. Pijpers, A. C. Antonio, J. de la C. Soto, and A. M. A. Calderón, "Life cycle assessment of a novel bipolar electro dialysis-based flow battery concept and its potential use to mitigate the intermittency of renewable energy generation," *J Energy Storage*, vol. 35, p. 102339, Mar. 2021, doi: 10.1016/J.EST.2021.102339.
- [55] Tanaka et al., "TRIVALENT AND TETRAVALENT MIXED WANADIUM COMPOUND PRODUCING METHOD AND WANADIUM ELECTROLYTE PRODUCING METHOD," 2003
- [56] ebm-papst St. Georgen GmbH & Co. KG, "Product data sheet 63142TDHHP." [Online]. Available: www.ebmpapst.com
- [57] G. M. G. J. H. R. H. M. J. O. et al. Hauschild M, "Recommendations for Life Cycle Impact Assessment in the European context - based on existing environmental impact assessment models and factors (International Reference Life Cycle Data System - ILCD handbook)," 2011.
- [58] H.-J. Althaus, R. Hischier, M. Osses EMPA, S. Gallen Alex Primas, S. Hellweg ETH Zürich Niels Jungbluth, and M. Chudacoff Chudacoff Ökoscience, "Swiss Centre for Life Cycle Inventories A joint initiative of the ETH domain and Swiss Federal Offices Life Cycle Inventories of Chemicals Data v2.0 (2007)," 2007. [Online]. Available: www.ecoinvent.org.
- [59] I. Iwakiri, T. Antunes, H. Almeida, J. P. Sousa, R. B. Figueira, and A. Mendes, "Redox flow batteries: Materials, design and prospects," *Energies (Basel)*, vol. 14, no. 18, Sep. 2021, doi: 10.3390/en14185643.